J|A|C|S
ARTICLES

Published on Web 04/09/2008

PEG-Detachable Polyplex Micelles Based on Disulfide-Linked Block Catiomers as Bioresponsive Nonviral Gene Vectors

Seiji Takae,[†] Kanjiro Miyata,[‡,⊥] Makoto Oba,[§] Takehiko Ishii,[‡,⊥] Nobuhiro Nishiyama,[∥,⊥] Keiji Itaka,[∥] Yuichi Yamasaki,[†,⊥] Hiroyuki Koyama,[§] and Kazunori Kataoka*[,†,‡,∥,⊥]

Department of Materials Engineering, Graduate School of Engineering, The University of Tokyo, 7-3-1 Hongo, Bunkyo-ku, Tokyo 113-8656, Japan, Department of Bioengineering, Graduate School of Engineering, The University of Tokyo, 7-3-1 Hongo, Bunkyo-ku, Tokyo 113-8656, Japan, Department of Clinical Vascular Regeneration, Graduate School of Medicine, The University of Tokyo, 7-3-1 Hongo, Bunkyo-ku, Tokyo 113-8655, Japan, Division of Clinical Biotechnology, Center for Disease Biology and Integrative Medicine, Graduate School of Medicine, The University of Tokyo, 7-3-1 Hongo, Bunkyo-ku, Tokyo 113-0033, Japan, and Center for NanoBio Integration, The University of Tokyo, 7-3-1 Hongo, Bunkyo-ku, Tokyo 113-8656, Japan

Received January 15, 2008; E-mail: Kataoka@bmw.t.u-tokyo.ac.jp

Abstract: PEG-based polyplex micelles, which can detach the surrounding PEG chains responsive to the intracellular reducing environment, were developed as nonviral gene vectors. A novel block catiomer, PEG-SS-P[Asp(DET)], was designed as follows: (i) insertion of biocleavable disulfide linkage between PEG and polycation segment to trigger PEG detachment and (ii) a cationic segment based on poly(aspartamide) with a flanking *N*-(2-aminoethyl)-2-aminoethyl group, P[Asp(DET)], in which the Asp(DET) unit acts as a buffering moiety inducing endosomal escape with minimal cytotoxicity. The polyplex micelles from PEG-SS-P[Asp(DET)] and plasmid DNA (pDNA) stably dispersed in an aqueous medium with a narrowly distributed size range of ~80 nm due to the formation of hydrophilic PEG palisades while undergoing aggregation by the addition of 10 mM dithiothreitol (DTT) at the stoichiometric charge ratio, indicating the PEG detachment from the micelles through the disulfide cleavage. The PEG-SS-P[Asp(DET)] micelles showed both a 1–3 orders of magnitude higher gene transfection efficiency and a more rapid onset of gene expression than PEG-P[Asp(DET)] micelles without disulfide linkages, due to much more effective endosomal escape based on the PEG detachment in endosome. These findings suggest that the PEG-SS-P[Asp(DET)] micelle may have promising potential as a nonviral gene vector exerting high transfection with regulated timing and minimal cytotoxicity.

Introduction

Successful gene therapy, which is a promising treatment for numerous intractable diseases, relies on the development of efficient gene vectors. Polyplexes formed by electrostatic interaction between plasmid DNA (pDNA) and cationic polymers (catiomers) have attracted much attention as a safe, versatile alternative to viral vectors.[1–7] A promising approach to realizing the polyplexes for in vivo gene delivery is the use of PEG-based block catiomers. These catiomers spontaneously associate with pDNA to form sub-100 nm polyplex micelles with a dense, hydrophilic PEG palisade surrounding the core.[8–11] These micelles show high colloidal stability under physiological conditions and substantial transfection activity against various cell types even after preincubation with serum proteins.[12,13] Moreover, polyplex micelles demonstrate prolonged blood circulation and in vivo gene transfer to the liver and tumor.[14–16]

[†] Department of Materials Engineering, The University of Tokyo.
[‡] Department of Bioengineering, The University of Tokyo.
[§] Department of Clinical Vascular Regeneration, The University of Tokyo.
[∥] Center for Disease Biology and Integrative Medicine, The University of Tokyo.
[⊥] Center for NanoBio Integration, The University of Tokyo.

(1) Pack, D. W.; Hoffman, A. S.; Pun, S.; Stayton, P. S. *Nat. Rev. Drug Discov.* **2005**, *4*, 581–593.
(2) Merdan, T.; Kopecek, J.; Kissel, T. *Adv. Drug Delivery Rev.* **2002**, *54*, 715–758.
(3) Wagner, E.; Meyer, M. *Hum. Gene Ther.* **2006**, *17*, 1062–1076.
(4) Kabanov, A. V. *Adv. Drug Delivery Rev.* **2006**, *58*, 1597–1621.
(5) Park, T. G.; Jeong, J. H.; Kim, S. W. *Adv. Drug Delivery Rev.* **2006**, *58*, 467–486.
(6) Osada, K.; Kataoka, K. *Adv. Polym. Sci.* **2006**, *202*, 113–153.
(7) Neu, M.; Fischer, D.; Kissel, T. *J. Gene Med.* **2005**, *7*, 992–1009.
(8) Katayose, S.; Kataoka, K. *Bioconjugate Chem.* **1997**, *8*, 702–707.
(9) Katayose, S.; Kataoka, K. *J. Pharm. Sci.* **1998**, *87*, 160–163.
(10) Ogris, M.; Brunner, S.; Schuller, S.; Kircheis, S.; Wagner, E. *Gene Ther.* **1999**, *6*, 595–605.
(11) Kwok, K. Y.; McKenzie, D. L.; Evers, D. L.; Rice, K. G. *J. Pharm. Sci.* **1999**, *88*, 996–1003.
(12) Itaka, K.; Yamauchi, K.; Harada, A.; Nakamura, K.; Kawaguchi, H.; Kataoka, K. *Biomaterials* **2003**, *24*, 4495–4506.
(13) Itaka, K.; Harada, A.; Nakamura, K.; Kawaguchi, H.; Kataoka, K. *Biomacromolecules* **2002**, *3*, 841–845.
(14) Harada-Shiba, M.; Yamauchi, K.; Harada, A.; Takanisawa, I.; Shimokado, K.; Kataoka, K. *Gene Ther.* **2002**, *9*, 407–414.
(15) Miyata, K.; Kakizawa, K.; Nishiyama, N.; Yamasaki, Y.; Watanabe, T.; Kohara, M.; Kataoka, K. *J. Controlled Release* **2005**, *109*, 15–23.

10.1021/ja800336v CCC: $40.75

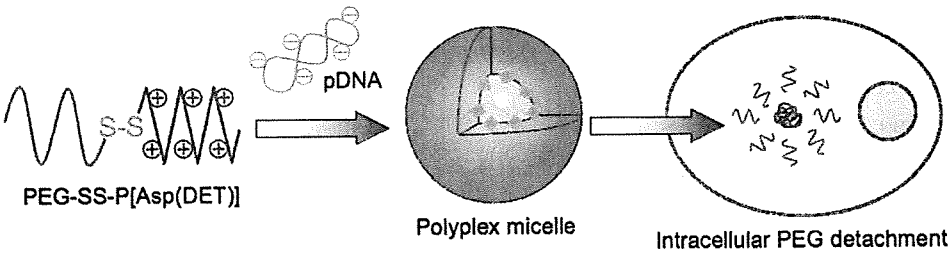

Figure 1. Schematic illustration of PEG-detachable polyplex micelle formation and the PEG detachment in the reducing intracellular environment.

We recently reported high transfection efficiency and low cytotoxicity with the use of polyplex micelles formed by PEG-*block*-poly(aspartamide) copolymers carrying the *N*-(2-aminoethyl)-2-aminoethyl group in the side chain (PEG-P[Asp(DET)]).[17] With regard to in vivo application, the polyplex micelles demonstrate appreciable gene transfer into vascular lesions without any vessel occlusion by thrombus[18] and bone regeneration of a mouse bone defect when transfected with genes coding for osteogenic factors.[19] These successful in vivo gene therapies have been explained by the specific structure of the side chain of P[Asp(DET)], in which the 1,2-ethanediamine moiety of the *N*-(2-aminoethyl)-2-aminoethyl group exhibits a distinct two-step protonation behavior, suggesting a potential proton sponge capacity of Asp(DET) units for efficient endo/lysosomal escape.[17]

However, polyplex micelles formed from PEG-P[Asp(DET)] could be further improved upon to achieve successful in vivo systemic therapies. P[Asp(DET)] homopolymer polyplexes show higher transfection efficiency than PEG-P[Asp(DET)] micelles especially at low charge ratios,[20] suggesting that the PEG palisade surrounding PEG-P[Asp(DET)] polyplex micelles would hamper the transfection. The decrease in gene transfection efficiency by PEGylation to catiomers (PEG dilemma) is also observed in previous work.[16,21,22] In addition, the time-dependent monitoring of gene expression against multicellular tumor spheroids reveals that the polyplex micelles from PEG-P[Asp(DET)] cause delayed gene expression, compared with polyplexes from cationic homopolymers.[20] This is sometimes undesired especially when rapid expression is required. On the other hand, the polyplexes from P[Asp(DET)] homocatiomers tend to aggregate through interactions with serum proteins,[18] suggesting limited in vivo application of the system without PEGylation. Although P[Asp(DET)] homocatiomers exhibited appreciably lower cytotoxicity compared with typical polycations such as polyethyleneimine (PEI),[23] PEGylation to P[Asp(DET)] further decreases the cytotoxicity to obtain successful transfection of primary cells.[17,18,20]

In order to overcome the aforementioned PEG dilemma, we designed here PEG detachable smart polyplex micelles sensitive to the intracellular environment as a smart gene vector (Figure 1). Block catiomers containing disulfide linkages between PEG and P[Asp(DET)] segments, PEG-SS-P[Asp(DET)], were synthesized to obtain this design goal (Scheme 1). Subsequent disulfide reduction of the block catiomer can occur during several steps of the endocytic pathway.[24] The cytoplasm and nuclear space are highly reducing environments due to abundant reduced glutathione (GSH) as well as redox enzymes such as the thioredoxin family. In addition, several studies suggest that disulfide bond reduction can begin on the exofacial surface of the cell and must continue after endocytosis. In this regard, involvement of plasma membrane-associated protein disulfide isomerase (PDI) is strongly implicated, as disulfide reduction is inhibited by an anti-PDI antibody and a PDI-inhibitor.[25,26] Moreover, NADH-oxidase (NOX) is reported as another cell surface-associated protein with disulfide−thiol interchange activity similar to PDI. Interestingly, the activity of this enzyme is constitutively activated in cancerous cells such as HeLa and hepatoma cells.[27] Finally, cysteine is actively transported from the cytoplasm to the lysosome lumen via a specific transporter in fibroblasts.[28]

Though the cleavage mechanism of the disulfide linkages cannot be predicted for the PEG-SS-P[Asp(DET)] micelle system utilized herein, the effect of PEG detachment on the gene transfection efficiency can be predicted based on where cleavage may occur. As a result of PEG detachment at the cell surface, the exposed cation segments may trigger a strong association to cells, increasing the cellular uptake of the micelles. Inside endosomes, the PEG detachment would cause the interaction between the exposed cation segments and the endosomal membrane and/or increase endosomal pressure, resulting in the destruction of the endosomal membrane to enable effective endosomal escape. In the cytoplasm and nucleus, the release of pDNA that forms the polyplex core might become smoother because steric repulsion disappears as the PEG cleaves, causing easier access of cellular polyanions to the complex core. Even if the reduction of disulfide linkages occurs in any of the steps outlined above, a more rapid alteration of gene expression and an increased transfection efficiency are expected.

(16) Kursa, M.; Walker, G. F.; Roessler, V.; Ogris, M.; Roedl, W.; Kircheis, R.; Wagner, E. *Bioconjugate Chem.* **2003**, *14*, 222–231.
(17) Kanayama, N.; Fukushima, S.; Nishiyama, N.; Itaka, K.; Jang, W.-D.; Miyata, K.; Yamasaki, Y.; Chung, U.-i.; Kataoka, K. *ChemMedChem* **2006**, *1*, 439–444.
(18) Akagi, D.; Oba, M.; Koyama, H.; Nishiyama, N.; Fukushima, S.; Miyata, T.; Nagawa, H.; Kataoka, K. *Gene Ther.* **2007**, *14*, 1029–1038.
(19) Itaka, K.; Ohba, S.; Miyata, K.; Kawaguchi, H.; Nakamura, K.; Takato, T.; Chung, U.-i.; Kataoka, K. *Mol. Ther.* **2007**, *15*, 1655–1662.
(20) Han, M.; Bae, Y.; Nishiyama, N.; Miyata, K.; Oba, M.; Kataoka, K. *J. Controlled Release* **2007**, *121*, 38–48.
(21) Brissault, B.; Kichler, A.; Leborgne, C.; Danos, O.; Cheradame, H.; Gau, J.; Auvray, L.; Guis, C. *Biomacromolecules* **2006**, *7*, 2863–2870.
(22) Sagara, K.; Kim, S. W. *J. Controlled Release* **2002**, *79*, 271–281.
(23) Masago, K.; Itaka, K.; Nishiyama, N.; Chung, U.-i.; Kataoka, K. *Biomaterials* **2007**, *28*, 5169–5175.
(24) Saito, G.; Swanson, J. A.; Lee, K.-D. *Adv. Drug Delivery Rev.* **2003**, *55*, 199–215.
(25) Feener, E. P.; Shen, W. C.; Ryser, H. J. *J. Biol. Chem.* **1990**, *265*, 18780–18785.
(26) Mandel, R.; Ryser, H. J.; Ghani, F.; Wu, M.; Peak, D. *Proc. Natl. Acad. Sci. U.S.A.* **1993**, *90*, 4112–4116.
(27) Morre, D. J.; Morre, D. M. *Free Radical Res.* **2003**, *37*, 795–808.
(28) Pisoni, R. L.; Acker, T. L.; Lisowski, K. M.; Lemons, R. M.; Thoene, J. G. *J. Cell Biol.* **1990**, *110*, 327–335.

Scheme 1. Synthetic Route of PEG-SS-P[Asp(DET)] Synthesis (Left) and the Chemical Structures of Control Polymers Used in This Experiment (PEG-P[Asp(DET)] and P[Asp(DET)]) (Right)

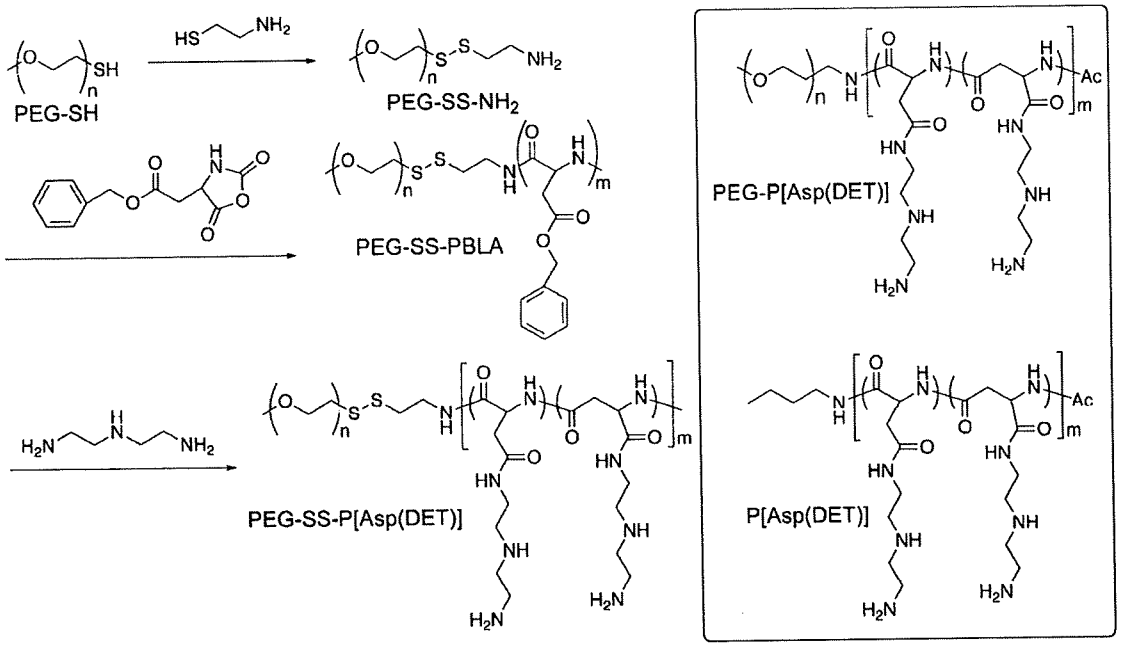

Based on such assumptions, we newly synthesized the PEG-SS-P[Asp(DET)] copolymer and prepared polyplex micelles sensitive to reducing environments. These micelles were expected to show comparable colloidal stability to PEG-P[Asp(DET)] micelles before cellular uptake, while, inside the cell, detachment of PEG would enable pDNA activity and alteration to gene expression. Therefore, careful characterization of both the PEG-SS-P[Asp(DET)] copolymer and the polyplex micelles was performed in regards to the reduction of disulfide linkages. In addition, the influence of the PEG detachment on the onset of gene expression and the mechanism of the disulfide reduction were evaluated through the time-dependent observation of the gene expression and the intracellular localization of pDNA.

Materials and Methods

Materials. α-Methoxy-ω-mercapto PEG (PEG-SH, M_n = 10000, M_w/M_n = 1.03) and β-benzyl-L-aspartate *N*-carboxyanhydride (BLA-NCA) were obtained from NOF Co. (Tokyo, Japan). Methanol (MeOH), 2-aminoethanethiol, benzene, acetonitrile, hexane, ethyl acetate, and D-luciferin were purchased from Wako Chemical Industries, Ltd. (Osaka, Japan). Dichloromethane, *N,N*-dimethylformamide (DMF), diethylenetriamine (DET), and *N*-methyl-2-pyrrolidone (NMP) were also purchased from Wako Chemical Industries and purified by distillation before use. A pGL3 control vector, which was purchased from Promega Co. (Madison, WI), was used as pDNA in all the experiments. This pDNA was amplified in competent DH5α *Escherichia coli* and purified using HiSpeed Plasmid MaxiKit purchased from QIAGEN Inc. (Valencia, CA). Water was purified using a Milli-Q instrument (Millipore, Bedford, MA).

Synthesis of PEG-SS-P[Asp(DET)]. As shown in Scheme 1, PEG-SH (1 g, 0.1 mmol) was dissolved in MeOH (100 mL), followed by the reaction with 2-aminoethanethiol (100 equiv to PEG-SH, 0.77 g, 10 mmol) at room temperature to obtain PEG-SS-NH_2. After a GPC peak due to PEG dimers (PEG-SS-PEG) generated by the side reaction disappeared, the reaction mixture was dialyzed against MeOH for 2 days and evaporated. Then, 80 mL of benzene were added, and the mixture was freeze-dried to obtain the white powder. To remove the PEG disulfide dimers (PEG-SS-PEG) generated during the dialysis, the powder dissolved in 30 mL of H_2O/CH_3CN (4:1) was loaded onto a CM Sephadex C-50 cation exchange chromatograph (GE Healthcare UK, Ltd., Little Chalf-ont, England), eluted with H_2O/CH_3CN (4:1) containing 0.125% NH_3. The eluate was evaporated and freeze-dried with distilled water to obtain the PEG-SS-NH_2 (570 mg, 57% yield). From gel permeation chromatography (GPC), M_n and M_w/M_n were determined to be 9880 and 1.02, respectively. The conversion to the aminoethanethiol moiety was confirmed to be quantitative (94%) based on the ^{1}H NMR data [CH_3 (3.2 ppm) and CH_2 (2.8 ppm)] (Figure S1) measured with a JEOL EX300 spectrometer (JEOL, Tokyo, Japan).

The PEG-SS-poly(β-benzyl L-aspartate) (PEG-SS-PBLA) copolymer was prepared by the ring opening polymerization of BLA-NCA (4.4 mmol, 1.1 g) in CH_2Cl_2/DMF (10:1, 15 mL) at 35 °C from the terminal primary amino group of PEG-SS-NH_2 (0.04 mmol, 400 mg).[29] The reaction mixture was precipitated into hexane/AcOEt (6:4). After filtration, the precipitate was dissolved in a small amount of CH_2Cl_2, followed by the addition of an excess amount of benzene, and lyophilized to obtain the white powder (910 mg, 61% yield). The degree of polymerization (DP) of PBLA was calculated to be 100 from ^{1}H NMR spectroscopy based on the peak intensity of benzyl protons of PBLA side chains (7.3 ppm) to the methylene protons of the PEG chain (3.6 ppm) (Figure S2).

Lyophilized PEG-SS-PBLA (130 mg) was dissolved in NMP (5.2 mL) at 27 °C, followed by the reaction with DET (2.3 mL, 50 equiv to benzyl group of PBLA segment) diluted in NMP (2.3 mL) under anhydrous conditions at 15 °C. After 15 min, the reaction mixture was slowly added dropwise into an aqueous solution of acetic acid (10% v/v, 40 mL) and dialyzed against a solution of 0.01 N HCl and, subsequently, distilled water (MWCO: 6–8000 Da). The final solution was lyophilized to obtain the polymer as the chloride salt form with a yield of 66% (104 mg). The structure of this block catiomer was confirmed by ^{1}H NMR and size-exclusion chromatography (SEC) [column: Superdex 200 10/300 GL (GE Healthcare UK, Ltd.); eluent: 10 mM Tris-HCl buffer + 500 mM NaCl (pH 7.4); flow rate: 0.75 mL/min; detector RI; ambient temperature].

(29) Harada, A.; Kataoka, K. *Macromolecules* **1995**, *28*, 5294–5299.

Preparation of PEG-SS-P[Asp(DET)]/pDNA Polyplex Micelles. The PEG-SS-P[Asp(DET)] block copolymer and pDNA were separately dissolved in 10 mM Tris-HCl buffer (pH 7.4). The polymer solution was added to a 2-times-excess volume of 50 μg/mL pDNA solution to form the polyplex micelles at various *N/P*, the residual molar ratio of the amino group in the block cationer to phosphate group in pDNA. The final concentration of pDNA in all the samples was adjusted to 33 μg/mL. The PEG-P[Asp(DET)] block copolymer (M_w = 39 000; DP of P[Asp(DET)] segment: 100) and P[Asp(DET)] (DP = 98) (Scheme 1) were used as controls, and their polyplexes were prepared in the same way as PEG-SS-P[Asp(DET)]/pDNA polyplex micelles.

Gel Retardation Assay. Polyplex solutions formed with pDNA (33 μg/mL) were diluted to 20 μg/mL with 10 mM Tris-HCl buffer and then electrophoresed at 100 V for 1 h on a 0.9 wt% agarose gel in 3.3 mM Tris-acetic acid buffer containing 1.7 mM sodium acetate. The migrated pDNA was visualized with ethidium bromide staining (0.5 μg/mL in deionized water).

Dynamic Light Scattering (DLS) Measurements. The size of the polyplexes was evaluated by DLS. Sample solutions with various *N/P* ratios in 10 mM Tris-HCl buffer (pH 7.4) were adjusted to have a pDNA concentration of 33 μg/mL. DLS measurements were carried out at 37 °C using a Zetasizer Nano-ZS instrument (Malvern Instruments, Malvern, UK), equipped with a He−Ne ion laser (λ = 633 nm) with a scattering angle of 90°.

Radiolabeling of pDNA and Cellular Uptake Study of the Polyplexes. pDNA was radioactively labeled with ^{32}P-dCTP using the Nick Translation System (Invitrogen Co., Carlsbad, CA). Unincorporated nucleotides were removed using the High Pure PCR Product Purification Kit (Roche Diagnostics Co., Indianapolis, IN). After the purification, 7 μg of labeled pDNA were mixed with 700 μg of nonlabeled pDNA. The polyplex and micelle samples were prepared by mixing the radioactive pDNA solution with each polymer solution (33 μg pDNA/mL). For the cellular uptake experiment, HeLa cells were seeded in Dulbecco's modified Eagle medium (DMEM) containing 10% fetal bovine serum (FBS) on 24-well tissue culture treated plates 24 h prior to experimentation. The cells were incubated with 30 μL of the radioactive polyplex solution (1 μg of pDNA/well) in 400 μL of DMEM containing 10% FBS. After 6 h of incubation, the cells were washed 3 times with PBS and lysed with 200 μL of cell culture lysis buffer (Promega, Co., Madison, WI). The lysates were mixed with 5 mL of scintillation cocktail, Ultima Gold (PerkinElmer, MA), and then, the radioactivity was measured using a liquid scintillation counter. The results are presented as a mean and standard deviation of the mean obtained from four samples.

In Vitro Transfection. HeLa cells were seeded on 24-well culture plates and incubated for 24 h in 400 μL of DMEM containing 10% FBS before transfection. The cells were then incubated with the polyplex micelles prepared from PEG-SS-P[Asp(DET)], PEG-P[Asp(DET)], and P[Asp(DET)] (30 μL, 1 μg of pDNA/well) with various *N/P* ratios in DMEM containing 10% FBS for 6 h, followed by an additional incubation for 42 h in the absence of polyplexes. The cells were washed in triplicate with 200 μL of Dulbecco's PBS and lysed by the addition of 400 μL/well of the Promega lysis buffer. Luciferase gene expression was evaluated using the Luciferase Assay System (Promega Co., Madison, WI) and a Lumat LB957 luminometer (Berthold Technologies Co., Bad Wildbad, Germany). The results were expressed as light units per milligram of cell protein determined by a BCA assay kit (PIERCE Biotechnology, Rockford, IL). The results are presented as a mean and standard deviation of the mean obtained from four samples.

Time-Dependent Monitoring of in Vitro Transfection. HeLa cells and 293T cells were seeded on 35-mm culture dishes and incubated for 24 h in 2 mL of DMEM containing 10% FBS before transfection. The cells were then incubated with the polyplex micelles prepared from PEG-SS-P[Asp(DET)], PEG-P[Asp(DET)], and P[Asp(DET)] (90 μL/dish, 3 μg of pDNA/dish) at *N/P* = 32 in DMEM containing 10% FBS. After 6 h, the medium was exchanged with fresh media containing 100 μM D-luciferin. The dishes were set in a luminometer incorporated in a small CO_2 incubator (AB-2550 Kronos Dio, ATTO Co., Tokyo, Japan), and the bioluminescence was monitored every 20 min (2 min collection time).

Confocal Laser Scanning Microscope (CLSM) Observation. pDNA was labeled with Cy5 using the Label IT Nucleic Acid Labeling Kit (Mirus, Madison, WI) according to the manufacture's protocol. HeLa cells were seeded on a 35-mm glass base dish (Iwaki, Japan) and incubated overnight in 1 mL of DMEM containing 10% FBS. After the medium was replaced with fresh medium, 90 μL of polyplex solution containing 3 μg of Cy5-labeled pDNA (*N/P* = 32) were applied. After 6 h of incubation, the medium was removed, the cells were washed twice with PBS, and fresh media was added. The intracellular distributions of the polyplex micelles were observed by CLSM following acidic late endosome and lysosome staining with LysoTracker Green (Molecular Probes, Eugene, OR). The CLSM observation was performed using LSM 510 (Carl Zeiss, Germany) with a 63× objective (C-Apochromat, Carl Zeiss, Germany) at excitation wavelengths of 488 nm (Ar laser) and 633 nm (He−Ne laser) for LysoTracker Green and Cy5, respectively. Colocalization of polyplex micelles in the late endosome and lysosome was quantified as follows:

Colocalization ratio = Cy5 pixels colocalization/Cy5 pixels total

where Cy5 pixels colocalization represents the number of pixels with Cy5 colocalizing with LysoTracker inside the cells and the Cy5 pixels total represents number of all pixels with Cy5 existing in the cells. The results are presented as a mean and standard error of the mean obtained from 10 cells.

Results and Discussion

Synthesis of PEG-SS-P[Asp(DET)]. A PEG-poly(aspartamide) block copolymer with a disulfide linkage between PEG and poly(aspartamide) was prepared as shown in Scheme 1. Initially, α-methoxy-ω-mercapto PEG (PEG-SH, M_n = 10 000) was reacted with 2-aminothanethiol in MeOH to introduce a primary amino group into PEG-SH via a disulfide linkage. The conversion ratio was confirmed to be 94% based on the ^{1}H NMR data (Figure S1). Then, β-benzyl L-aspartate *N*-carboxyanhydride (BLA-NCA) was polymerized in CH_2Cl_2/DMF at 35 °C by an initiation from the terminal primary amino group of PEG-SS-NH_2. The degree of polymerization (DP) of PBLA was calculated to be 100 from ^{1}H NMR spectroscopy, and GPC measurement revealed that the obtained PEG-SS-PBLA showed a unimodal molecular weight distribution (Figure S2). The aminolysis of PEG-SS-PBLA in NMP in the presence of a molar excess of diethylenetriamine (DET, 50 equiv relative to benzyl groups) was carried out. The ^{1}H NMR spectrum of the obtained polymer (Figure S3) reveals that the introduction of DET into the side chains of PBLA was almost quantitative (98.5%) in spite of the extremely short reaction time (15 min) and relatively low temperature (15 °C). The detailed mechanism of this unique aminolysis reaction of PBLA was reported elsewhere.[30] Size-exclusion chromatography (SEC) measurements revealed a unimodal molecular weight distribution of the obtained polymer (Figure 2, line 1), suggesting a minimal occurrence of inter- or intrapolymer cross-linking by DET during aminolysis. To confirm the presence of disulfide linkages between PEG and polycation segments, SEC measurement was done after the addition of 10 mM dithiothreitol (DTT) to the PEG-SS-P[Asp(DET)] solution. In the SEC chromatogram, two overlapping peaks (Figure 2, line 2) were observed at elution times extremely similar to those for PEG-SH (Figure 2, line 3) and

(30) Nakanishi, M.; Park, J.-S.; Jang, W.-D.; Oba, M.; Kataoka, K. *React. Funct. Polym.* **2007**, *67*, 1361–1372.

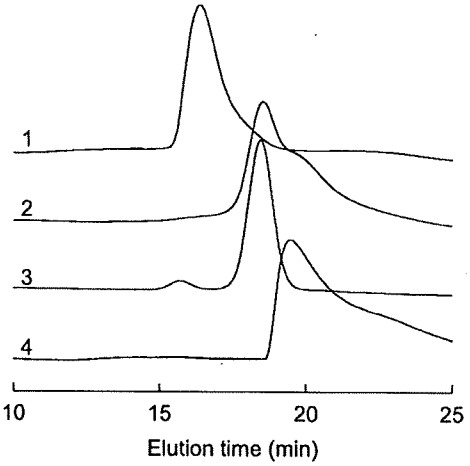

Figure 2. SEC charts of PEG-SS-P[Asp(DET)] (line 1), PEG-SS-P[Asp(DET)] after 4 h incubation with 10 mM DTT (line 2), PEG-SH (line 3), and P[Asp(DET)] (line 4).

P[Asp(DET)] (Figure 2, line 4), indicating that the obtained polymer was linked via a disulfide linkage between PEG and P[Asp(DET)] segments.

Formation of Polyplex Micelles from pDNA and PEG-SS-P[Asp(DET)]. Polyplex micelles were prepared by mixing each polymer solution with the pDNA solution at various *N/P* ratios. In order to demonstrate polyplex formation between PEG-SS-P[Asp(DET)] and pDNA, a gel electrophoresis retardation assay was performed using 0.9 wt % agarose gel. A PEG-P[Asp(DET)] block copolymer without the disulfide linkage and P[Asp(DET)] homocatiomer were used as controls (Scheme 1). As shown in Figure 3, the band of free pDNA disappeared at $N/P > 2$ in all of the samples, indicating successful and complete polyplex formation between pDNA and the three catiomers. This is stoichiometrically consistent with the monoprotonated form of the ethylenediamine unit in PEG-P[Asp(DET)] and P[Asp(DET)] at pH 7.4.[17,20] The diameters of the polyplexes or the polyplex micelles prepared at different *N/P* ratios are shown in Figure 4a. The diameters of the polyplex micelles from PEG-P[Asp(DET)] and PEG-SS-P[Asp(DET)] were determined to be 80–90 nm throughout the examined *N/P* ratios (1–16). On the other hand, the polyplexes from P[Asp(DET)] formed large aggregates with a size of approximately 600 nm specifically at *N/P* ~2. Considering that zeta-potential of the P[Asp(DET)] polyplex was close to neutral at $N/P = 2$ (Figure S4), the aggregation was presumably due to the formation of charge stoichiometric complexes showing lower electrostatic repulsion among the polyplexes. The system of PEG-SS-P[Asp(DET)] and PEG-P[Asp(DET)] did not show such aggregation, indicating a high colloidal stability due to the steric repulsion of the PEG palisades of the shell.[31]

Reducing Environment-Sensitive Cleavage of the Disulfide Linkages of the Polyplex Micelles from PEG-SS-P[Asp(DET)]. To confirm the detachment of PEG from the PEG-SS-P[Asp(DET)] polyplex micelles, the diameter of the micelles ($N/P = 2$) was monitored after the addition of 10 mM DTT, as a model reaction for the reducing environment of the cytoplasm. As shown in Figure 4b, 10 mM DTT rapidly induced an increase in size of PEG-SS-P[Asp(DET)] micelles, whereas, in the case of control

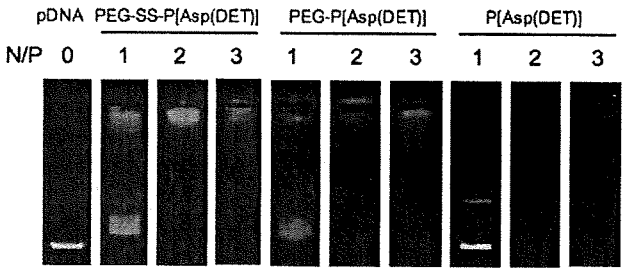

Figure 3. Gel retardation assay of the polyplexes.

micelles from PEG-P[Asp(DET)], such a size increase was not observed, indicating that the PEG chains on the PEG-SS-P[Asp(DET)] micelles were detached due to the cleavage of the disulfide bond. Moreover, as a model of the extracellular environment, the polyplex micelles were incubated in 10 μM DTT, which is an effective 50-fold molar equivalent of the PEG-SS-P[Asp(DET)] within the micelles. As a result, the polyplex micelles did not show increased size (Figure 4b), indicating that the PEG detachment would be dependent on the concentration of the surrounding thiol groups. To check the PEG detachment at other *N/P* ratios, the ζ-potential of the polyplex micelles was measured in the absence or presence of 10 mM DTT. The polyplexes from PEG-SS-P[Asp(DET)] and PEG-P[Asp(DET)] were observed to have ζ-potentials with a very small absolute value (~4 mV) in $N/P > 2$ (Figure S4), suggesting that the polyplexes from the PEG-*b*-catiomers form a core–shell micellar architecture with a hydrophilic and neutral PEG shell surrounding the polyplex core. After the addition of 10 mM DTT, the ζ-potential of PEG-SS-P[Asp(DET)] polyplex micelles shifted to a positive value (~28 mV) comparable to that of the P[Asp(DET)] polyplexes. On the other hand, there was no change in the ζ-potential of PEG-P[Asp(DET)] micelles by the addition of DTT. These results indicate that, regardless of *N/P* ratio, the surface-covered PEG chains detached from the PEG-SS-P[Asp(DET)] polyplex micelles when present in a reducing environment.

Cellular Uptake Study. Though the PEG-SS-P[Asp(DET)] polyplex micelles were responsive to reducing environments, it is significant to determine where the PEG chains will be detached after contact with cells. Rice et al. concluded that the complexes formed from PEG(5 kDa)-SS-Lys_{18} and pDNA showed more in vitro cellular uptake than PEG-Lys_{18} complexes without disulfide linkages, suggesting partial reduction of the disulfide linkages outside cells.[32] To confirm that the disulfide linkages were cleaved either outside or inside cells, polyplexes with ^{32}P-radiolabeled pDNA were prepared and the uptake to human cervical carcinoma HeLa cells was measured. As shown in Figure 5, PEG-SS-P[Asp(DET)] and PEG-P[Asp(DET)] polyplex micelles showed a minimal uptake into the cells, with only ~0.5% of the total dose being taken up. In contrast, 2–4% of P[Asp(DET)] polyplexes were taken into the cells, probably due to the electrostatic association between the positive charge of the polyplexes and the negative charge of the plasma membrane. If the disulfide linkages were reduced prior to uptake by cells, a higher percentage of the PEG-SS-P[Asp(DET)] micelles would be taken up than the PEG-P[Asp(DET)] micelles. In contrast, the cellular uptakes of PEG-P[Asp(DET)] and PEG-SS-P[Asp(DET)] micelles are equivalent, suggesting that the

(31) Kataoka, K.; Harada, A.; Nagasaki, Y. *Adv. Drug Delivery Rev.* **2001**, *47*, 113–131.

(32) Kwok, K. Y.; McKenzie, D. L.; Evers, D. L.; Rice, K. G. *J. Pharm. Sci.* **1999**, *88*, 996–1003.

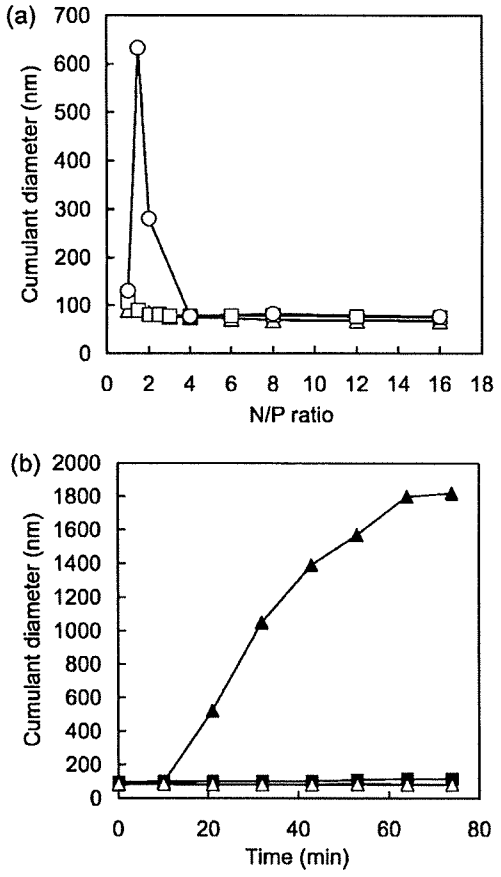

Figure 4. (a) Size of the polyplexes from PEG-SS-P[Asp(DET)] (△), PEG-P[Asp(DET)] (□), and P[Asp(DET)] (○). (b) Time-dependent change of the size of PEG-SS-P[Asp(DET)] polyplex micelles at *N/P* = 2 with 10 mM DTT (▲) and with 10 μM DTT (△), and PEG-P[Asp(DET)] polyplex micelles with 10 mM DTT (■).

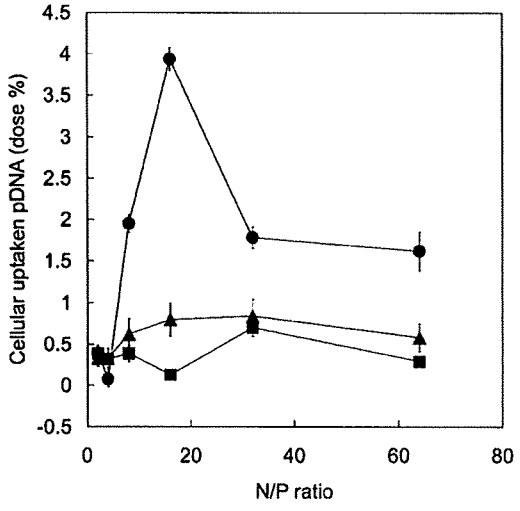

Figure 5. Cellular uptake of pDNA complexed with catiomers; PEG-SS-P[Asp(DET)] (▲), PEG-P[Asp(DET)] (■), and P[Asp(DET)] (●). ^{32}P-labeled pDNA polyplexes were incubated with HeLa cells in DMEM containing 10% FBS at 37 °C for 6 h. The amount of internalized pDNA is represented as a percentage for the dosed pDNA (1 μg/well).

PEG-SS-P[Asp(DET)] micelles maintain their PEG palisade structure under normal culture conditions for at least 6 h. Note

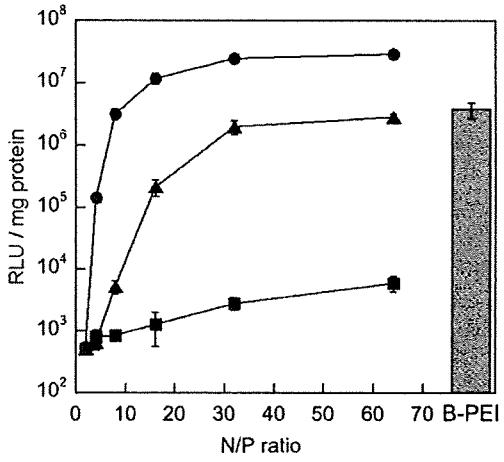

Figure 6. In vitro transfection of the luciferase gene into HeLa cells by polyplexes from PEG-SS-P[Asp(DET)] (▲), PEG-P[Asp(DET)] (■), and P[Asp(DET)] (●) with varying *N/P* ratios. Branched polyethyleneimine (B-PEI, 25 kDa) at *N/P* = 32 was shown as a control (gray bar). The cells were incubated with each polyplex in DMEM containing 10% FBS for 6 h, followed by incubation for a further 42 h in the absence of the polyplexes. Transfection is reported in relative light units (RLU) per mg of protein.

that there is a decrease in cellular uptake of the P[Asp(DET)] polyplexes with *N/P* ≥ 32. This may be due to inhibition of uptake by free catiomers which are not associated with the polyplexes.

In Vitro Transfection Efficiency and Cytotoxicity. The in vitro transfection efficiency of these polyplexes with HeLa cells was assessed using a luciferase assay. Based on the cellular uptake study, cells were incubated with the polyplexes for 6 h, followed by a 42 h incubation after medium replacement. As shown in Figure 6, PEG-SS-P[Asp(DET)] polyplex micelles showed 2–3 orders of magnitude higher transfection efficiency than the PEG-P[Asp(DET)] polyplex micelles at *N/P* ≥ 16, which is comparable to branched polyethyleneimine (B-PEI, 25 kDa). It is surprising that the introduction of disulfide linkages to the block catiomers remarkably increased the transfection efficiency, though the efficiency was somewhat less than P[Asp(DET)] polyplexes. Low cytotoxicity together with high transfection efficiency is an extremely important aspect for nonviral gene vectors. The cytotoxicity of the polyplexes was evaluated with the same cell culture procedure as the transfection, followed by the CellTiter-Glo luminescent cell viability assay. Polyplex micelles from PEG-SS-P[Asp(DET)], PEG-P[Asp(DET)], and P[Asp(DET)] polyplexes showed more than 90% cell viability in all *N/P* ratios tested in this study, while B-PEI polyplexes induced a significant decrease in cell viability (~40%) at *N/P* = 64 (Figure S5). A similar tendency was observed at lower *N/P* as well in the case of longer incubation times and higher doses (data not shown). These results indicate that P[Asp(DET)] and the block catiomers would be desirable as in vivo gene vectors due to their high transfection efficiency as well as low toxicity.

Mechanism of the High Transfection Efficiency of PEG-SS-P[Asp(DET)] Micelles. It is important to understand where the disulfide linkages of the PEG-SS-P[Asp(DET)] polyplex micelles are cleaved inside the cell. Therefore, the time-dependent profile of transfection efficiency was monitored with AB-2550 Kronos Dio (ATTO Co. Ltd., Tokyo, Japan), which is a luminometer incorporated into a small CO_2 incubator, allowing continuous measurement of bioluminescence by transfected

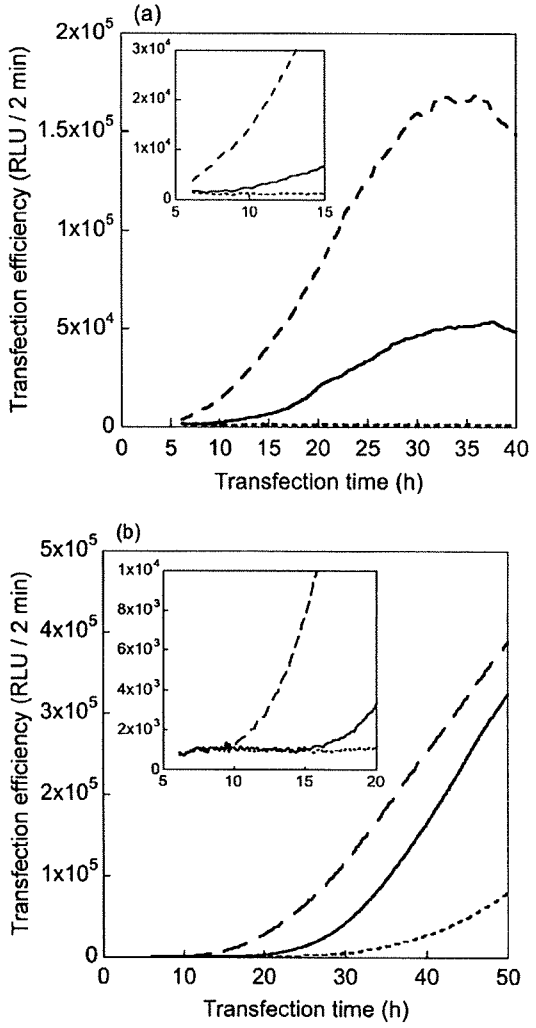

Figure 7. Time-dependent profiles of transfection efficiency against HeLa cells (a) and 293T cells (b) induced by PEG-SS-P[Asp(DET)] (solid line), PEG-P[Asp(DET)] (dotted line), and P[Asp(DET)] (dashed line) polyplexes at $N/P = 32$. The cells were incubated with each polyplex in DMEM containing 10% FBS for 6 h, followed by incubation in DMEM containing 10% FBS and 100 μM D-luciferin in the absence of polyplexes. The time shown in the x-axis started from the addition of polyplex solutions and the measurement started from 6 h. The inserts are expanded figures from 5 to 15 h (a) and from 5 to 20 h (b).

cells. After HeLa cells were incubated with the polyplexes for 6 h, the medium modified to include luciferin was used to culture the cells and bioluminescence from expressed luciferase was monitored at 20 min intervals. As shown in Figure 7a, the gene expression induced by P[Asp(DET)] polyplexes started to be observed immediately after the medium replacement (at 6 h), while the expression by PEG-SS-P[Asp(DET)] micelles started at 11 h and increased remarkably after 16 h. A similar tendency of delayed expression with PEG-SS-P[Asp(DET)] micelle carriers compared with P[Asp(DET)] polyplexes was observed with 293T cells as well (Figure 7b). The reason of the delayed expression of PEG-SS-P[Asp(DET)] micelles is presumably related to the process of the disulfide reduction inside the cell. In addition, clear expression by PEG-SS-P[Asp(DET)] micelles in 293T cells was observed 10 h earlier than PEG-P[Asp(DET)] micelles, probably due to the detachment of PEG chains. These results indicate that PEG-SS-P[Asp(DET)] micelles could regulate the onset of the gene expression, which is a significantly attractive characteristic in this system.

In order to gain more insight into the relationship between the cleavage of disulfide linkages and transfection efficiency, intracellular trafficking of pDNA in the micelles was observed with a confocal laser scanning microscope (CLSM), using PEG-SS-P[Asp(DET)] polyplex micelles with Cy5-labeled pDNA (red) at $N/P = 32$. LysoTracker (green) was used as an endo/lysosomal marker. As shown in Figure 8a, Cy5-pDNA of the polyplex micelles from PEG-P[Asp(DET)] and PEG-SS-P[Asp(DET)] associates to the plasma membrane 6 h after transfection, whereas the red fluorescence from P[Asp(DET)] polyplexes seemed to spread out from the green fluorescence of LysoTracker even at 6 h, indicating fast endosomal escape. This result would correspond to the transfection profile (Figure 7a) where transfection by P[Asp(DET)] polyplexes is observed starting at 6 h. Figure 8b shows CLSM images after 6 h of incubation with the polyplex and 6 h postincubation in the absence of polyplexes, corresponding to the time when a gene expression by PEG-SS-P[Asp(DET)] micelles started (12 h in Figure 7a). In these images, the pDNA of PEG-P[Asp(DET)] micelles is colocalized and sequestered in the endo/lysosome, resulting in the absence of expression in Figure 7a. On the other hand, the pDNA of PEG-SS-P[Asp(DET)] micelles spread out from LysoTracker, indicating that the PEG-SS-P[Asp(DET)] micelles that escaped from the endosome would be capable of inducing gene expression. In the case of P[Asp(DET)] polyplexes, pDNA spread out from endo/lysosome increased remarkably. Time-dependent colocalization of pDNA in the endo/lysosomes was quantified and is shown in Figure 8c. PEG-P[Asp(DET)] micelles exhibited high colocalization even after 2 days, while less colocalization was observed in the PEG-SS-P[Asp(DET)] system, suggesting a more effective endosomal escape. A similar localization profile of pDNA in the PEG-SS-P[Asp(DET)] system was observed in 293T cells (Figure S6). Considering the transfection profile as well as CLMS images (Figure 7 and 8), it is likely that cleavage of the disulfide linkages of PEG-SS-P[Asp(DET)] micelles occurs in the endocytic pathway, resulting in effective endosomal escape probably due to interaction between the exposed polycation segments and endosomal membrane, and/or increased osmotic pressure in the endosome induced by detached PEG chains. As a result, the gene expression onset of PEG-SS-P[Asp(DET)] micelles was intermediate when compared with P[Asp(DET)] polyplexes and PEG-P[Asp(DET)] micelles. There is an issue that disulfide reduction in the endosome would be disfavored due to the low GSH concentration as well as the acidic environment inducing protonation of thiol groups and decreased reactivity of thiol–disulfide oxidoreductase (e.g., PDI, thioredoxin, etc.) because these enzymes typically exhibit optimal activity around neutral pH. Nevertheless, Low et al. directly observed images of disulfide cleavage with FRET technology using folate–SS–rhodamine conjugates.[33] In addition, calcein-loaded polymersome formed from a PEG-SS-poly(propylene sulfide) block copolymer showed the rapid release of calcein inside the endosome due to the disulfide reduction, facilitating endosomal rupture.[34] In the case of the PEG-SS-P[Asp(DET)] system, considering the increased endosomal escape, not all PEG chains but a substantial fraction of them are assumed to be detached

(33) Yang, J.; Chen, H.; Vlahov, I. R.; Cheng, J.-X.; Low, P. S. *Proc. Natl. Acad. Sci. U.S.A.* **2006**, *103*, 13872–13877.
(34) Cerritelli, S.; Velluto, D.; Hubbell, J. A. *Biomacromolecules* **2007**, *8*, 1966–1972.

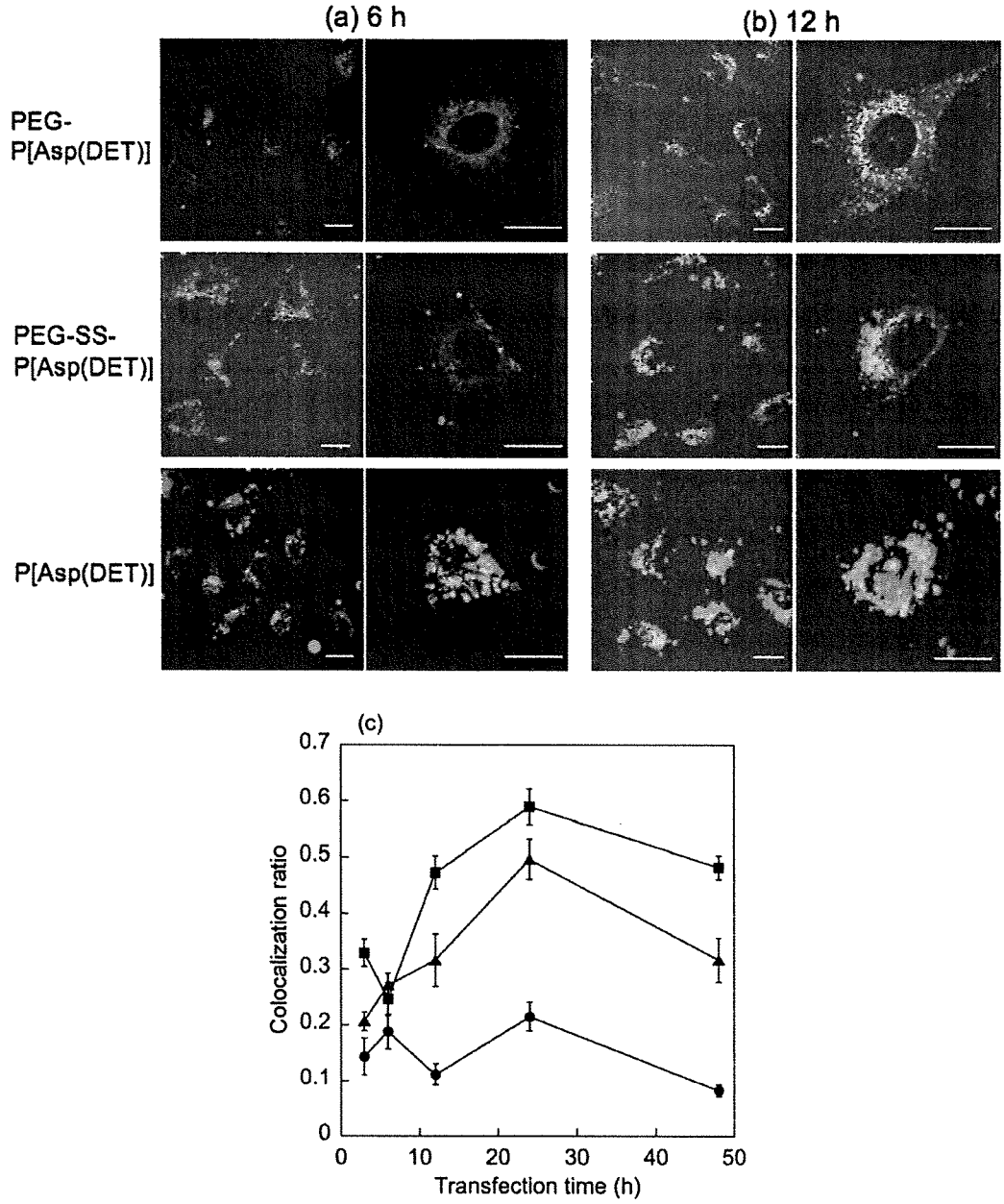

Figure 8. (a, b) Intracellular distribution of pDNA challenged by PEG-P[Asp(DET)] and PEG-SS-P[Asp(DET)] micelles, and P[Asp(DET)] polyplexes at $N/P = 32$. The complexes loaded with Cy5-labeled pDNA (red) were incubated with HeLa cells for 6 h, followed by incubation in the absence of polyplexes. The CLSM observation was performed 6 h (a) and 12 h (b) after transfection, using a 63× objective. The acidic late endosome and lysosome were stained with LysoTracker Green (green). The scale bar represents 20 μm. (c) Quantitative results of colocalization profile of Cy5-labeled pDNA in late endosome and lysosome transfected by PEG-P[Asp(DET)] (■), PEG-SS-P[Asp(DET)] (▲), and P[Asp(DET)] (●) polyplexes.

in the endocytic pathway as a result of disulfide reduction. In the future, further mechanistic investigations of the disulfide cleavage will be performed to reveal a detailed relationship between PEG detachment and gene transfection efficiency, contributing to establishing the design criteria for smart polyplex micelles useful for in vivo transfection studies.

Conclusion

We newly synthesized a disulfide-linked block catiomer, PEG-SS-P[Asp(DET)], to develop a PEG detachable polyplex micelle sensitive to an intracellular reducing environment. This micelle showed several orders of magnitude higher gene transfection efficiency than a micelle without disulfide linkages in spite of the similar level of their cellular uptakes. Moreover, gene expression induced by the PEG-SS-P[Asp(DET)] micelle started between the expression onsets of the P[Asp(DET)] polyplex and PEG-P[Asp(DET)] micelle, indicating that the PEG-SS-P[Asp(DET)] micelle could regulate the onset of the gene expression. CLSM images revealed that this transfection behavior of the PEG-SS-P[Asp(DET)] micelle could be explained by effective endosomal escape due to the PEG detachment in the endosome. As this micelle overcame the PEG dilemma, it would be highly promising for in vivo application to exert spatio-temporal regulated transfection with minimal cytotoxicity.

Acknowledgment. The authors acknowledge Mr. Shigeto Fukushima, the University of Tokyo, for his advice about polymer synthesis. This study was financially supported by the Core Research for Evolutional Science and Technology (CREST) from the Japan Science and Technology Agency (JST) and also by a grant for the 21st Century COE Program "Human-Friendly Materials based on Chemistry" from the Ministry of Education, Culture, Sports, Science and Technology of Japan (MEXT). S.T. would like to express his special gratitude for the scholarship from the Asahi Glass Scholarship Foundation.

Supporting Information Available: ^{1}H NMR spectra and GPC charts of PEG-SS-NH_2, PEG-SS-PBLA and PEG-SS-P[Asp-(DET)], ζ-potential measurements, cytotoxicity study, and CLSM images of 293T cells. These materials are available free of charge via the Internet at http://pubs.acs.org.

JA800336V

Journal of the American Chemical Society

Article

Polyplexes from Poly(aspartamide) Bearing 1,2-Diaminoethane Side Chains Induce pH-Selective, Endosomal Membrane Destabilization with Amplified Transfection and Negligible Cytotoxicity

Kanjiro Miyata, Makoto Oba, Masataka Nakanishi, Shigeto Fukushima, Yuichi Yamasaki, Hiroyuki Koyama, Nobuhiro Nishiyama, and Kazunori Kataoka

J. Am. Chem. Soc., **2008**, 130 (48), 16287-16294 • Publication Date (Web): 12 November 2008

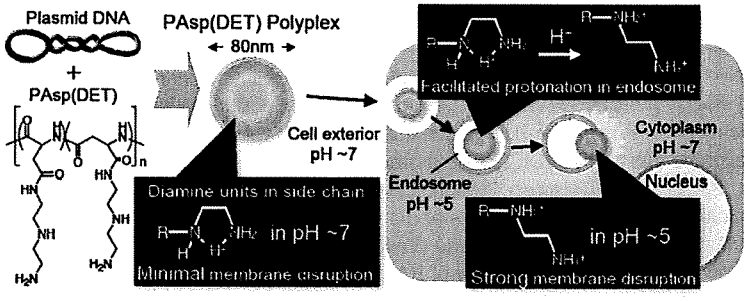

More About This Article

Additional resources and features associated with this article are available within the HTML version:

- Supporting Information
- Access to high resolution figures
- Links to articles and content related to this article
- Copyright permission to reproduce figures and/or text from this article

View the Full Text HTML

Journal of the American Chemical Society is published by the American Chemical Society. 1155 Sixteenth Street N.W., Washington, DC 20036

J|A|C|S
ARTICLES

Published on Web 11/12/2008

Polyplexes from Poly(aspartamide) Bearing 1,2-Diaminoethane Side Chains Induce pH-Selective, Endosomal Membrane Destabilization with Amplified Transfection and Negligible Cytotoxicity

Kanjiro Miyata,[†,‡] Makoto Oba,[§] Masataka Nakanishi,[∥] Shigeto Fukushima,[⊥] Yuichi Yamasaki,[∥,‡] Hiroyuki Koyama,[§] Nobuhiro Nishiyama,[⊥,‡] and Kazunori Kataoka*[,†,∥,⊥,‡]

Department of Bioengineering and Department of Materials Engineering, Graduate School of Engineering, and Center for NanoBio Integration, The University of Tokyo, 7-3-1 Hongo, Bunkyo-ku, Tokyo 113-8656, Japan, Department of Clinical Vascular Regeneration, Graduate School of Medicine, The University of Tokyo, 7-3-1 Hongo, Bunkyo-ku, Tokyo 113-8655, Japan, and Center for Disease Biology and Integrative Medicine, Graduate School of Medicine, The University of Tokyo, 7-3-1 Hongo, Bunkyo-ku, Tokyo 113-0033, Japan

Received June 23, 2008; E-mail: kataoka@bmw.t.u-tokyo.ac.jp

Abstract: Polyplexes assembled from poly(aspartamide) derivatives bearing 1,2-diaminoethane side chains, [PAsp(DET)] display amplified in vitro and in vivo transfection activity with minimal cytotoxicity. To elucidate the molecular mechanisms involved in this unique function of PAsp(DET) polyplexes, the physicochemical and biological properties of PAsp(DET) were thoroughly evaluated with a control bearing 1,3-diaminopropane side chains, PAsp(DPT). Between PAsp(DET) and PAsp(DPT) polyplexes, we observed negligible physicochemical differences in particle size and ζ-potential. However, the one methylene variation between 1,2-diaminoethane and 1,3-diaminopropane drastically altered the transfection profiles. In sharp contrast to the constantly high transfection efficacy of PAsp(DET) polyplexes, even in regions of excess polycation to plasmid DNA (pDNA) (high N/P ratio), PAsp(DPT) polyplexes showed a significant drop in the transfection efficacy at high N/P ratios due to the progressively increased cytotoxicity with N/P ratio. The high cytotoxicity of PAsp(DPT) was closely correlated to its strong destabilization effect on cellular membrane estimated by hemolysis, leakage assay of cytoplasmic enzyme (LDH assay), and confocal laser scanning microscopic observation. Interestingly, PAsp(DET) revealed minimal membrane destabilization at physiological pH, yet there was significant enhancement in the membrane destabilization at the acidic pH mimicking the late endosomal compartment (pH ~5). Apparently, the pH-selective membrane destabilization profile of PAsp(DET) corresponded to a protonation change in the flanking diamine unit, i.e., the monoprotonated gauche form at physiological pH and diprotonated anti form at acidic pH. These significant results suggest that the protonated charge state of 1,2-diaminoethane may play a substantial role in the endosomal disruption. Moreover, this novel approach for endosomal disruption neither perturbs the membranes of cytoplasmic vesicles nor organelles at physiological pH. Thus, PAsp(DET) polyplexes, residing in late endosomal or lysosomal states, smoothly exit into the cytoplasm for successful transfection without compromising cell viability.

Introduction

Successful transfection with polycation-based gene vectors (polyplexes) significantly depends on the chemical structure of the incorporated polycations.[1,2] Polyethylenimine (PEI) and its derivatives display protonation of amino groups over a wide pH range. Following polyplex formation, these well-known polycations exert a high transfection efficacy through endosomal escape supported by the proton sponge hypothesis.[3,4] However, there remains a great concern for the availability of PEI-based polyplexes in translational research, mainly due to their problematic toxicity.[5,6] Thus, the rational design of a polyplex system exhibiting clinically relevant gene expression with minimal toxicity remains an urgent complication for clinical

[†] Department of Bioengineering.
[‡] Center for NanoBio Integration.
[§] Department of Clinical Vascular Regeneration.
[∥] Department of Materials Engineering.
[⊥] Center for Disease Biology and Integrative Medicine.

(1) Pack, D. W.; Hoffman, A. S.; Pun, S.; Stayton, P. S. *Nature Rev. Drug Discovery* **2005**, *4*, 581–593.
(2) Mastrobattista, E.; van der Aa, M. A. E. M.; Hennink, W. E.; Crommelin, D. J. A. *Nature Rev. Drug Discovery* **2006**, *5*, 115–121.
(3) Boussif, O.; Lezoualc'h, F.; Zanta, M. A.; Mergny, M. D.; Scherman, D.; Demeneix, B.; Behr, J. *Proc. Natl. Acad. Sci. U.S.A.* **1995**, *92*, 7297–7301.
(4) Neu, M.; Fischer, D.; Kissel, T. *J. Gene Med.* **2005**, *7*, 992–1009.
(5) Fischer, D.; Li, Y.; Ahlemeyer, B.; Krieglstein, J.; Kissel, T. *Biomaterials* **2003**, *24*, 1121–1131.
(6) Moghimi, S. M.; Symonds, P.; Murray, J. C.; Hunter, A. C.; Debska, G.; Szewczyk, A. *Mol. Ther.* **2005**, *11*, 990–995.

10.1021/ja804561g CCC: $40.75

extension of nonviral gene vectors. To overcome polycationic toxicity, a promising strategy is the incorporation of hydrophilic and nonionic poly(ethylene glycol) (PEG) to shield the deleterious, excess cationic charge associated with these carriers. Indeed, PEGylated polyplexes (polyplex micelles) formed through the association of PEG−polycation copolymers with DNA[7−12] were biocompatible under in vivo conditions, leading to appreciable in vivo gene expression with lower toxic effects.[13−16]

Nevertheless, further improvements in polyplex micelle systems are needed to show higher transfection efficacy and lower cytotoxicity for clinical translation. This recurring and pervasive problem endures, thereby motivating studies devoted to modulate the micellar, polycationic structure for effective clinical application in human gene therapy. Recently, we found that a flanking benzyl ester group of PEG-*b*-poly(β-benzyl L-aspartate) (PBLA) underwent a quantitative aminolysis reaction with a variety of amine compounds under a very mild condition,[17] allowing us to prepare an N-substituted poly(aspartamide) (PAsp) derivative library possessing a variety of cationic side chains from a single platformed PBLA.[18−25] A series of transfection and cytotoxicity assays of polyplexes prepared from the N-substituted PAsp derivative library revealed a highly promising candidate, PEG-*b*-poly{*N*-[*N*-(2-aminoethyl)-2-aminoethyl]aspartamide} (PEG−PAsp(DET)). A 1,2-diaminoethane unit was introduced as a side chain into PEG-*b*-PAsp, forming PEG-*b*-PAsp(DET); a series of primary cells and cultured cell lines were transfected, and significant gene expression with limited cytotoxicity was obtained. PEG−*b*-PAsp(DET) displayed high transfection efficacy comparable to commercially available linear PEI (ExGen 500) and the lipid-based system (Lipofectamine 2000); moreover, cytotoxicity levels were substantially lower compared to the controls.[15,16,19,21−25] Furthermore, PEG−PAsp(DET) polyplex micelles were successfully transfected in two animal models: (i) a rabbit's clamped carotid artery with neointima via intra-arterial injection[15] and (ii) a mouse skull by regulated release from a calcium phosphate cement scaffold to induce bone regeneration through the differentiation factor transduction.[16] The success of PEG−PAsp(DET) gene delivery in vivo has been attributed to the unique 1,2-diaminoethane structure in the side chain, where the *N*-(2-aminoethyl)-2-aminoethyl group exhibits a distinctive two-step protonation behavior. This dual protonation state suggests a strong pH-buffering capacity of Asp(DET) units for efficient endosomal escape.[19,21] Nevertheless, it still remains unknown whether the protonation behavior provides the crucial factor for excellent transfection when incorporated with PEG−PAsp. In parallel, it is unclear whether the low cytotoxicity of PEG−PAsp(DET) polyplex micelles is related to the particular cationic structure of Asp(DET) or simply due to the biocompatible PEG outer layer of the polyplex micelles.

These issues motivated us to clarify the structural factor of PAsp(DET) on transfection efficacy as well as cytocompatibility for additional polycationic structures successful for human gene therapy. To properly address the many architectural and chemical contributions of PEG−PAsp(DET), the following poly(aspartamides) were employed: (i) PAsp(DET) homopolymers to elucidate the effect of Asp(DET) units without PEGylation and (ii) a poly(aspartamide) bearing 1,3-diaminopropane units in the side chain as a control for 1,2-diaminoethane units, poly{*N*-[*N*-(3-aminopropyl)-3-aminopropyl]aspartamide} [PAsp(DPT)]. PAsp(DPT) exhibited a protonation degree over 88% at physiological pH and was considered to have a weak proton sponge effect. The high protonated state of Asp(DPT) at physiological pH is explained by the lowered electrostatic repulsion between the protonated diamine side chain units by the additional methylene group compared to Asp(DET). Detailed analysis of cellular membrane destabilization by PAsp(DET) and PAsp(DPT) revealed the distinct behavior of PAsp(DET) to facilitate membrane destabilization at the acidic pH of late endosomal or lysosomal states. This pH-selective membrane destabilization allows endosomal escape of PAsp(DET) polyplexes into the cytoplasm with limited toxicity to the other cytoplasmic membranes lying at neutral pH.

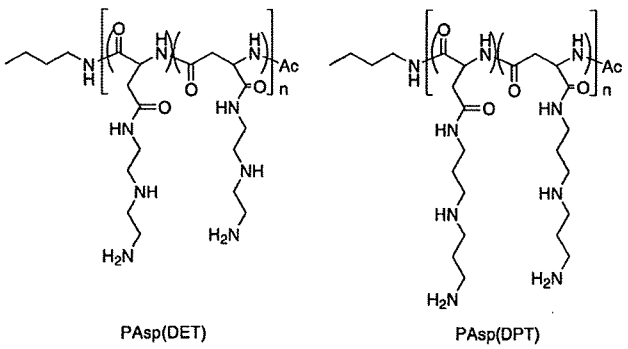

Results and Discussion

Protonation Degree (α) and Apparent pK_a of PAsp(DET) and PAsp(DPT). Previous studies revealed that a high transfection efficacy of PEI-based polyplexes was ascribed to their efficient endosomal escape, possibly due to the increased

(7) Kakizawa, Y.; Kataoka, K. *Adv. Drug Delivery Rev.* **2002**, *54*, 203–222.
(8) Katayose, S.; Kataoka, K. *Bioconjugate Chem.* **1997**, *8*, 702–707.
(9) Wolfert, M. A.; Schacht, E. H.; Toncheva, V.; Ulbrich, K.; Nazarova, O.; Seymour, L. W. *Human Gene Ther.* **1996**, *10*, 2123–2133.
(10) Choi, Y. H.; Liu, F.; Kim, J.; Choi, Y. K.; Park, J. S.; Kim, S. W. *J. Controlled Release* **1998**, *54*, 39–48.
(11) Vinogradov, S. V.; Bronich, T. K.; Kabanov, A. V. *Bioconjugate Chem.* **1998**, *9*, 805–812.
(12) Blessing, T.; Kursa, M.; Holzhauser, R.; Kircheis, R.; Wagner, E. *Bioconjugate Chem.* **2001**, *12*, 529–537.
(13) Harada-Shiba, M.; Yamauchi, K.; Harada, A.; Takamisawa, I.; Shimokado, K.; Kataoka, K. *Gene Ther.* **2002**, *9*, 407–414.
(14) Miyata, K.; Kakizawa, Y.; Nishiyama, N.; Yamasaki, Y.; Watanabe, T.; Kohara, M.; Kataoka, K. *J. Controlled Release* **2005**, *109*, 15–23.
(15) Akagi, D.; Oba, M.; Koyama, H.; Nishiyama, N.; Fukushima, S.; Miyata, T.; Nagawa, H.; Kataoka, K. *Gene Ther.* **2007**, *14*, 1029–1038.
(16) Itaka, K.; Ohba, S.; Miyata, K.; Kawaguchi, H.; Nakamura, K.; Takato, T.; Chung, U.; Kataoka, K. *Mol. Ther.* **2007**, *15*, 1655–1662.
(17) Nakanishi, M.; Park, J.-S.; Jang, W.-D.; Oba, M.; Kataoka, K. *React. Funct. Polym.* **2007**, *67*, 1361–1372.
(18) Fukushima, S.; Miyata, K.; Nishiyama, N.; Kanayama, N.; Yamasaki, Y.; Kataoka, K. *J. Am. Chem. Soc.* **2005**, *127*, 2810–2811.
(19) Kanayama, N.; Fukushima, S.; Nishiyama, N.; Itaka, K.; Jang, W.-D.; Miyata, K.; Yamasaki, Y.; Chung, U.; Kataoka, K. *ChemMedChem.* **2006**, *1*, 439–444.
(20) Arnida,; Nishiyama, N.; Kanayama, N.; Jang, W.-D.; Yamasaki, Y.; Kataoka, K. *J. Controlled Release* **2006**, *115*, 208–215.
(21) Han, M.; Bae, Y.; Nishiyama, N.; Miyata, K.; Oba, M.; Kataoka, K. *J. Controlled Release* **2007**, *121*, 38–48.
(22) Miyata, K.; Fukushima, S.; Nishiyama, N.; Yamasaki, Y.; Kataoka, K. *J. Controlled Release* **2007**, *122*, 252–260.
(23) Masago, K.; Itaka, K.; Nishiyama, N.; Chung, U.; Kataoka, K. *Biomaterials* **2008**, *28*, 5169–5175.
(24) Takae, S.; Miyata, K.; Oba, M.; Ishii, T.; Nishiyama, N.; Itaka, K.; Yamasaki, Y.; Koyama, H.; Kataoka, K. *J. Am. Chem. Soc.* **2008**, *130*, 6001–6009.
(25) Lee, Y.; Miyata, K.; Oba, M.; Ishii, T.; Fukushima, S.; Han, M.; Koyama, H.; Nishiyama, N.; Kataoka, K. *Angew. Chem., Int. Ed.* **2008**, *47*, 5163–5166.

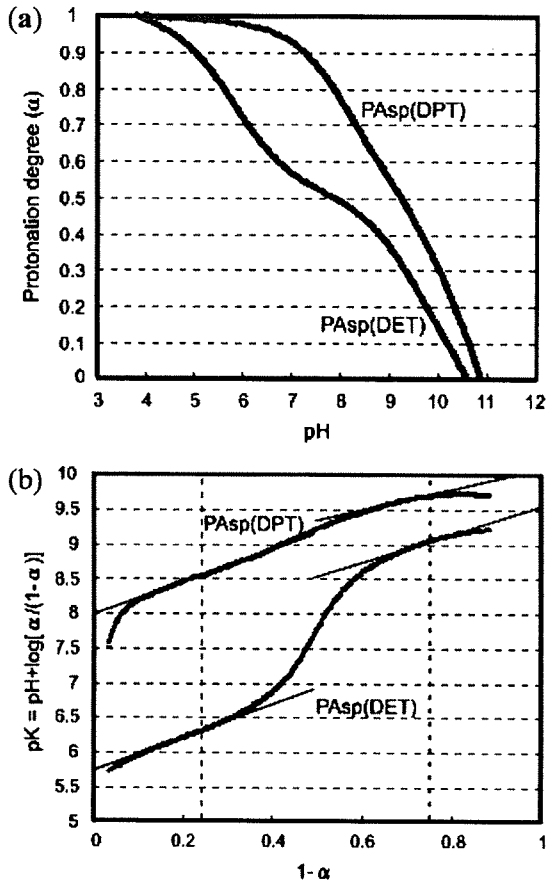

Figure 1. Protonation behavior of PAsp(DET) and PAsp(DPT). (a) Change in protonation degree (α) with pH (α/pH curve) (150 mM NaCl, 37 °C). (b) Change in apparent pK with 1 − α [pK/(1 − α) curve].

osmotic pressure caused by facilitated protonation of polycations in endosomal acidic compartments (the proton sponge effect).[3,4] Hence, the difference in the protonation degree between neutral pH and endosomal acidic pH (from 7.4 to 5.0) has been considered to be a crucial factor for successful transfection with polycation-based systems. In this regard, the α of PAsp(DET) and PAsp(DPT) was estimated from the potentiometric titration, which was monitored over the range of pH 2.3−12 in the 150 mM NaCl solution at 37 °C, mimicking the physiological condition. As shown in Figure 1a, the α/pH curves calculated from the obtained titration curves (data not shown) revealed that the protonation behavior of the cationic poly(aspartamides) fairly depended on the number of methylene groups between the primary and secondary amino groups in the side chain. PAsp(DET) exhibited a substantial change in the α from neutral pH 7.4 to acidic pH 5.0 due to a distinctive two-step protonation behavior; i.e., 37% increase in the α through the pH drop from 7.4 to 5.0. In contrast, PAsp(DPT) showed facilitated protonation typically at physiological pH, and consequently, the increase in the α by changing pH from 7.4 to 5.0 was only 10%, an approximately 4 times smaller value than that expected for PAsp(DET). These results indicate that PAsp(DET) has potentially higher buffering capacity in endosomal acidic compartments than PAsp(DPT).

From the distinctive two-step protonation behavior of PAsp(DET), it is reasonably concluded that the first and the second protonation in the side chain proceeds separately. The remarkable difference in the protonation behavior between PAsp(DET)

Scheme 1. Two-Step Protonation of the 1,2-Diaminoethane Moiety in the Side Chain of PAsp(DET)

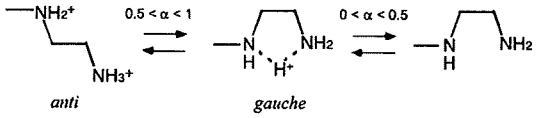

and PAsp(DPT) in the region of 0.5 < α < 1 indicates that the 1,2-diaminoethane unit in PAsp(DET) has restricted second protonation compared to the 1,3-diaminopropane unit in PAsp(DPT). The pK (=pH + log[α/(1 − α)]) values of PAsp(DET) and PAsp(DPT) were then calculated and plotted against 1 − α. Figure 1b clearly displays that PAsp(DET) has a substantially lower pK value in the range of 0 < 1 − α < 0.5, corresponding to the second protonation, than PAsp(DPT). Herein, apparent pK_a values in the first and the second protonations were defined as pK_{a1} (α = 0.25) and pK_{a2} (α = 0.75), respectively, and eventually were determined as follows: p$K_{a1,DET}$ = 9.1 and p$K_{a2,DET}$ = 6.3 for PAsp(DET), and p$K_{a1,DPT}$ = 9.7 and p$K_{a2,DPT}$ = 8.6 for PAsp(DPT). Although a large difference was not observed for K_{a1}, 2 orders of magnitude difference was observed for K_{a2}. It is worth noting that p$K_{a2,DET}$ was much lower than p$K_{a1,DET}$, indicating that the diprotonated form of the PAsp(DET) side chain suffers a thermodynamic penalty, presumably due to the electrostatic repulsion between two charged amino groups in the 1,2-diaminoethane moiety. The available conformation may be limited to an anti form according to three-bond interaction, i.e., butane effect, as shown in Scheme 1 to minimize the steric as well as electrostatic repulsion. As a result, the 1,2-diaminoethane side chain in PAsp(DET) takes a monoprotonated form at physiological pH (α = 0.53 at pH 7.4) as calculated from Figure 1a. Alternatively, addition of a single, hydrophobic methylene group in 1,3-diaminopropane units reduces the repulsion between the charged amino groups to increase the conformational freedom, leading to the smooth second protonation in PAsp(DPT) (α = 0.88 at pH 7.4). Note that both the 1,2-diaminoethane and 1,3-diaminopropnae, in PAsp(DET) and PAsp(DPT), respectively, may prefer to take the gauche conformation at the monoprotonated state, which is supported from the molecular orbital calculation.[26,27]

Preparation and Characterization of Polyplexes from PAsp(DET) and PAsp(DPT). The polyplex formation of PAsp(DET) and PAsp(DPT) was confirmed by agarose gel electrophoresis. The free pDNA band disappeared at N/P = 2 and 1.5 for PAsp(DET) and PAsp(DPT), respectively, indicating that all the pDNA molecules were associated with the polycations in the electrophoregram (Supporting Figure 2, Supporting Information). To quantitatively evaluate the relationship between N/P ratio and pDNA complexation with cationic PAsp(DET) and PAsp(DPT), an EtBr exclusion assay was completed. In this assay, pDNA complexation prevents EtBr molecules from intercalating into pDNA, resulting in the decrease in the EtBr fluorescence. Indeed, the EtBr fluorescence decreased with the increase in N/P ratios (Figure 2a), indicating the progressive complexation of pDNA with the polycations forming polyplexes. Also, Figure 2a exhibits that the inflection points of the fluorescence intensity are at N/P = 2 for PAsp(DET) and 1.4 for PAsp(DPT). These inflection points are in good agreement

(26) Corte, D. D.; Schelapfer, C.-W.; Daul, C. *Theor. Chem. Acc.* **2000**, *105*, 39–45.
(27) Bouchoux, G.; Choret, N.; Berruyer-Penaud, F. *J. Phys. Chem. A* **2001**, *105*, 3989–3994.

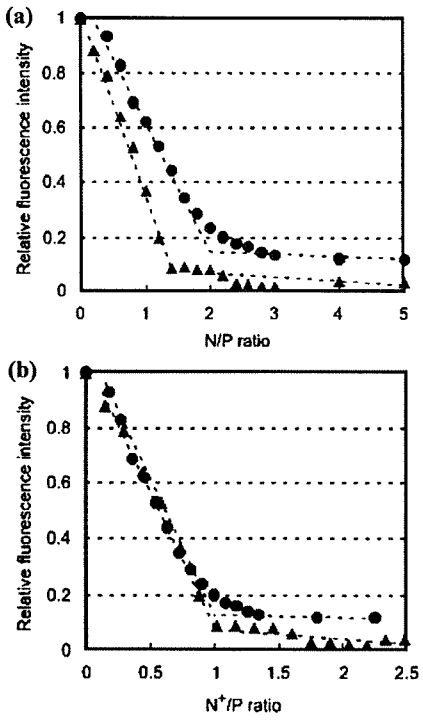

Figure 2. Ethidium bromide exclusion assay on PAsp(DET) and PAsp(DPT) polyplexes. (a) Relative fluorescence intensity vs N/P ratio. (b) Relative fluorescence intensity vs N^+/P ratio: (●) PAsp(DET) and (▲) PAsp(DPT).

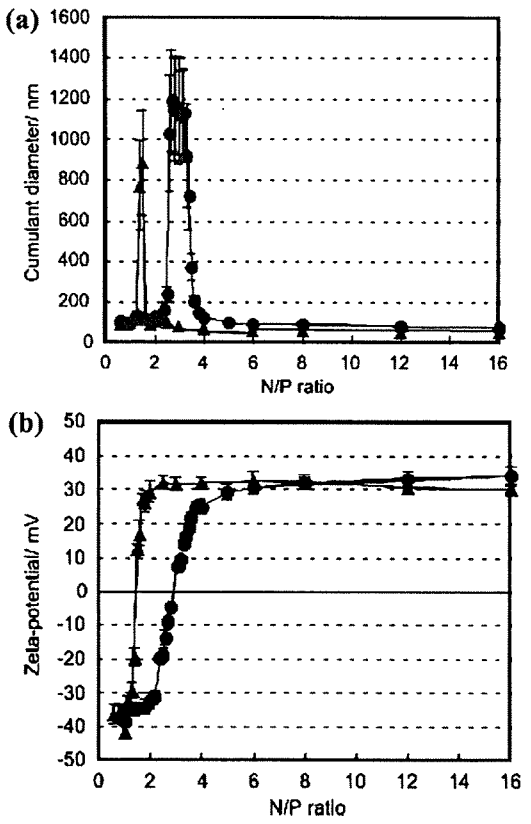

Figure 3. Change in the size and the ζ-potential of PAsp(DET) and PAsp(DPT) polyplexes with N/P ratio. (a) Cumulant diameter and (b) ζ-potential: (●) PAsp(DET), (▲) PAsp(DPT). All the samples were normalized to a concentration of 33 μg pDNA/mL at 37 °C. Results were expressed as mean ± SEM (n = 3).

with the N/P ratio where the free pDNA band disappeared from the electrophoregram (Supporting Figure 2, Supporting Information). These fluorescence data were replotted against N^+/P ratios, which were defined as the molar ratio of protonated amino groups at pH 7.4 in the polycations to phosphate groups in pDNA, as seen in Figure 2b. Note that the protonation degree of the amino groups of PAsp(DET) and PAsp(DPT) was determined to be 0.45 and 0.73 at pH 7.4, respectively, from the titration results without NaCl (data not shown). Obviously, both systems had the coincident inflection point of the fluorescence intensity at the N^+/P of unity, being consistent with the polyion-coupling between a phosphate group and an amino group in the protonated form expected from the α/pH curves. This result suggests that the pK_a value of PAsp(DET) shows minimal change with the polyplex formation, probably due to the thermodynamic penalty in diprotonated form of Asp(DET) units due to strong three-bond interaction (butane effect) caused by electrorepulsive interaction between two protonated amino groups.

The size and ζ-potential of polyplexes from PAsp(DET) and PAsp(DPT) in 10 mM Tris-HCl buffer (pH 7.4) were measured at 37 °C. As shown in Figure 3a, each polyplex had the critical range in N/P ratios, e.g., 2.5−3.5 and 1.4−1.5 for PAsp(DET) and PAsp(DPT), respectively, to reveal an appreciably large size of approximately 1000 nm. Considering that the ζ-potential of each polyplex was close to neutral in this critical range of N/P ratios, as seen in Figure 3b, these large-sized polyplexes may form through the secondary aggregation of the charge stoichiometric polyplexes showing minimal force of electrostatic repulsion. In the range over these critical N/P ratios, the size of both polyplexes were maintained <100 nm. The polyplexes in this range exhibited almost constant positive ζ-potential values (+30 mV) in both systems.

Transfection Efficacy and Cytotoxicity of PAsp(DET) and PAsp(DPT) Polyplexes. The transfection efficacy of the luciferase gene against a human hepatocyte cell line (Huh-7) and a human umbilical vein endothelial cell (HUVEC) was compared between PAsp(DET) and PAsp(DPT) polyplexes. The polyplexes prepared at N/P ratios of 4, 8, and 16 were examined in this assay, having almost the same size and ζ-potential (Figure 3a,b). Polyplexes prepared from branched polyethylenimine (BPEI) (25 kDa) were used as a control. As seen in Figure 4a,b, the highest transfection efficacy in both cells was achieved by the PAsp(DET) polyplexes prepared at the N/P ratio of 16. This transfection efficacy of PAsp(DET) polyplexes was 1 order of magnitude higher than that of BPEI polyplexes against HUVEC. Obviously, the transfection efficacy of PAsp(DET) polyplexes was enhanced with the increase in N/P ratio against both cells. On the contrary, PAsp(DPT) exhibited the decrease in the transfection efficacy with the increase in N/P ratio. Considering that the large difference was not observed in the size and ζ-potential between PAsp(DET) and PAsp(DPT) polyplexes (Figure 3a,b), this opposite trend in transfection profiles of these two polyplexes against N/P ratio is likely to be due to the distinctive physicochemical properties directly related to the difference in the chemical structures, particularly the side chain structures. Interestingly, in the region of low N/P ratio, the PAsp(DPT) polyplexes revealed a comparable transfection efficacy to PAsp(DET) polyplexes, even though the former was expected to exert substantially weaker buffering capacity than the latter, as judged from the α/pH curve (Figure 1a).

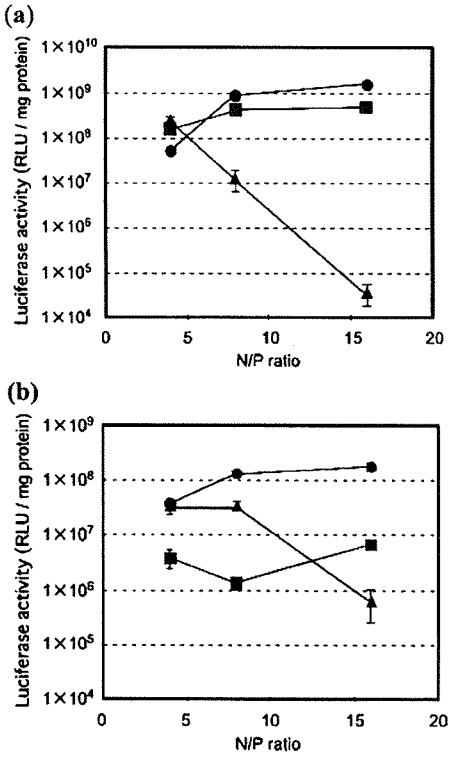

Figure 4. In vitro transfection of Huh-7 (a) and HUVEC (b) with PAsp(DET), PAsp(DPT), and BPEI polyplexes at varying N/P ratios evaluated by luciferase assays: (●) PAsp(DET), (▲) PAsp(DPT), and (■) BPEI. Results were expressed as mean ± SEM (n = 4).

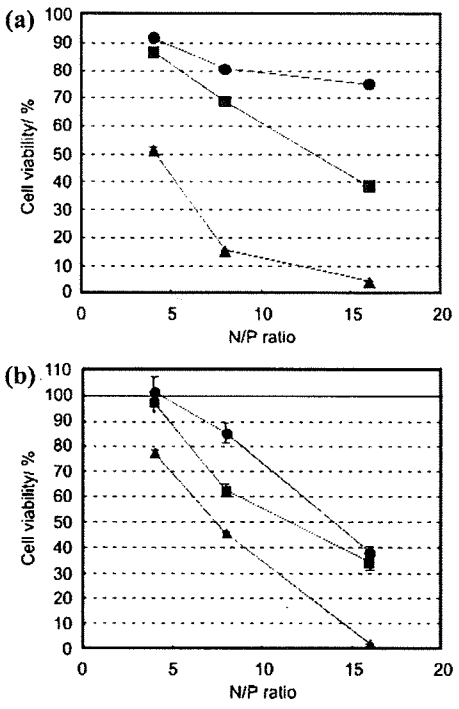

Figure 5. MTT cytotoxicity of Huh-7 (a) and HUVEC (b) with PAsp(DET), PAsp(DPT), and BPEI polyplexes evaluated under the same experimental conditions as in Figure 4 (luciferase assay): (●) PAsp(DET), (▲) PAsp(DPT), and (■) BPEI. Results were expressed as mean ± SEM (n = 4).

There are several key steps in the transfection process of an exogenous gene, such as cellular uptake, intracellular trafficking, release of the gene from the complexes, transcription, and translation. Furthermore, excess polycationic charge with polyplexes is an issue to induce impaired cellular homeostasis, resulting in the negative influences on whole transfection steps, especially transcription and translation. Indeed, our previous study revealed that the challenge of linear PEI polyplexes into Huh-7 cells stably expressing firefly luciferase highly impaired the transcription and translation processes to reduce the expression of firefly luciferase as well as a variety of house-keeping genes.[23] In this regard, a toxicological assay was completed to explore the different transfection profiles between PAsp(DET) and PAsp(DPT) polyplexes against N/P ratio. As shown in Figure 5a,b, the results of the MTT cell viability assay, the cytotoxicity of each polyplex under the same experimental condition as the luciferase assay increased with N/P ratio for both cells, Huh-7 and HUVEC. This result is in good agreement with the result from the MTT assay of each polymer without pDNA (Supporting Figure 3a,b and Supporting Table 1, Supporting Information). Obviously, the PAsp(DET) polyplex had much lower toxicity than the PAsp(DPT) polyplex. In detail, at a N/P ratio of 16 in Huh-7 cells, the viability of cells incubated with PAsp(DET) polyplexes was over 70% of that of control cells, whereas the viability was less than 10% in the case of PAsp(DPT) polyplexes (Figure 5a). Similarly, the cytotoxicity of PAsp(DPT) polyplexes was the highest against HUVEC, followed by BPEI and PAsp(DET) polyplexes (Figure 5b). From these results, it is worth noting that only one additional methylene group between two amino groups in the side chain crucially elevates the cytotoxicity of the cationic poly(aspartamides). This high cytotoxicity of PAsp(DPT) might contribute to the dramatically decreased transfection efficacy of PAsp(DPT) polyplexes at high N/P ratios. In contrast, cytotoxicity was substantially lowered in PAsp(DET) polyplexes, allowing high transfection efficacy with the increased N/P ratio.

To explore the endosomal escaping behavior of PAsp(DET) and PAsp(DPT) polyplexes, HUVEC trafficking studies were completed with a confocal laser scanning microscope (CLSM). In this experiment, pDNA was labeled by Cy5 (red), and nucleus and late-endosome/lysosome were stained by Hoechst 33342 (blue) and LysoTracker (green), respectively. Figure 6a,e shows the intracellular distribution of BPEI polyplexes 3 and 12 h after administration, respectively, as a positive control exerting an endosomal escaping function. Obviously, the red regions surrounding the yellow regions, where Cy5-labeled pDNA was localized in late-endosomes or lysosomes, were widely observed over time. It may be reasonable to judge that these spreading red regions represent the distribution of polyplexes exiting from the late endosomal or lysosomal stage into the cytoplasm. On the contrary, the negative control, PLys polyplexes, which lack significant buffering capacity, displayed much less red regions (Figure 6d,h), suggesting the segregation of Cy5-labeled pDNA in endo/lysosomal compartments without diffusing into cytoplasm. The confocal images of the cells transfected by PAsp(DET) polyplexes (Figure 6b,f) display spreading red regions into the cytoplasm, comparable to the previously described BPEI transfection. These data indicate facilitated transport of Cy5-labeled pDNA into the cytoplasm from the endo/lysosomal compartments. The CLSM images of PAsp(DET) polyplexes are consistent with the high buffering capacity of the native polymer. Interestingly, similar diffusing red regions were also observed for PAsp(DPT) polyplexes (Figure 6c,g), suggesting that PAsp(DPT) may facilitate endosomal escape of the polyplex, despite the previously determined poor pH-buffering capacity of PAsp(DPT). Indeed, PAsp(DPT) polyplexes showed

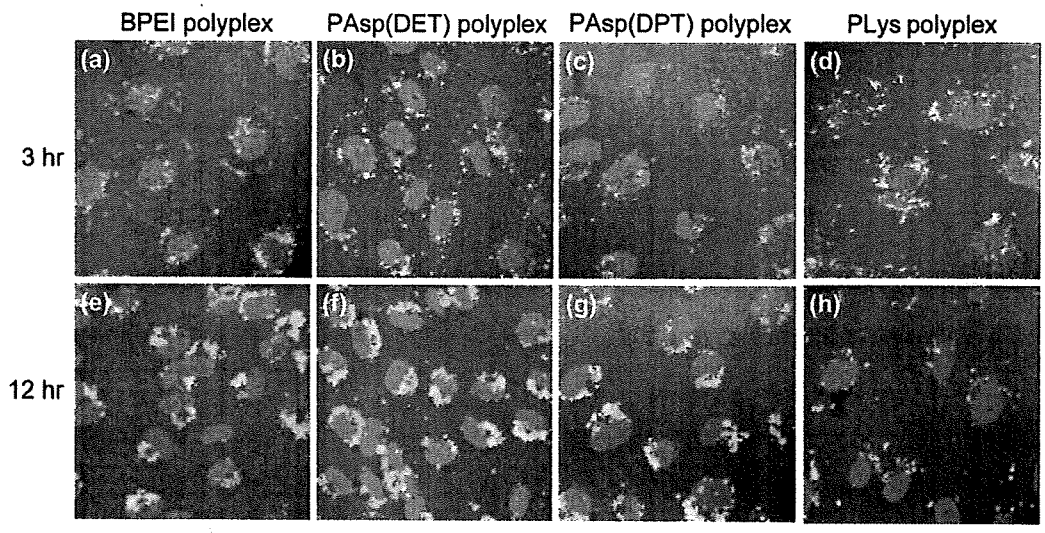

Figure 6. Intracellular distribution of Cy5-labeled pDNA complexed with a variety of polycations in HUVEC. Cy5-labeled pDNA and LysoTracker as a late-endosome and lysosome marker were observed in red and green, respectively. The cells were incubated at 37 °C for a definite time period, followed by washing with PBS, and subjected to CLSM imaging. Panels a–d and e–h are the images after 3 and 12 h incubation, respectively. (a and e) BPEI polyplexes (N/P = 8), (b and f) PAsp(DET) polyplexes (N/P = 8). (c and g) PAsp(DPT) polyplexes (N/P = 8). (d and h) PLys polyplexes (N/P = 2).

comparable transfection efficacy to BPEI and PAsp(DET) polyplexes at low N/P ratios (Figure 4a,b). These results strongly suggest the presence of another mechanism facilitating late endosomal or lysosomal escape beyond the putative proton sponge effect. Note that the medium change at 1 h after the polyplex administration significantly decreased the red regions (or dots) corresponding to endosomal escaping behavior in BPEI, PAsp(DET), and PAsp(DPT) (Supporting Figure 4, Supporting Information). This indicates that prolonged incubation of excess polyplexes with cells substantially facilitates the endosomal escape. Prolonged incubation should lead to the increased cellular uptake of polyplexes, presumably resulting in the polyplex accumulation with higher concentration in late-endosomal compartments to bring facilitated endosomal escape.

Membrane Destabilization by PAsp(DET) and PAsp(DPT). As described in the preceding section, the CLSM observation of Cy5-labeled pDNA in the intracellular compartment demonstrated that cytoplasmic transport efficiently occurred even for PAsp(DPT) polyplexes, known to possess the low buffering capacity. Of note, the previous studies addressed the destabilization of cellular membranes through the direct interaction with polycations,[5,6,28] possibly leading to the facilitated cytoplasmic transport of the polyplexes.[29–31] This destabilizing effect of polycations on the cellular membrane is considered to be dependent on the concentration (or N/P ratio), molecular weight, cationic charge density, and molecular structure of polycations.[5] Thus, the membrane destabilization induced by PAsp(DET) and PAsp(DPT) was estimated by the hemolysis assay, in which the amount of hemoglobin liberated from erythrocytes was determined from colorimetric analysis at 575 nm (Figure 7). Figure 7a clearly shows the significant difference in hemolytic activity between PAsp(DET) and PAsp(DPT) after an overnight incubation with murine erythrocytes at pH 7.4. The hemolytic activity of PAsp(DET) was negligible under the examined conditions, whereas PAsp(DPT) exhibited appreciable hemolytic activity in a concentration-dependent manner. Next, the hemolytic assays were repeated under acidic conditions indicative of the late endosomal or lysosomal state. Since overnight incubation of murine erythrocytes at pH 5.5 led to an appreciable decrease in the signal-to-noise ratio (Abs 575 nm), possibly due to instability of erythrocytes or conformational change of hemoglobins under the acidic condition, a shorter incubation time of 3 h was adopted. As clearly seen in Figure 7b, hemolytic activity levels were concentration-dependent for PAsp(DPT), regardless of the environmental pH. In direct contrast, however, the hemolytic activity of PAsp(DET) was critically enhanced by decreasing the environmental pH from 7.4 to 5.5 (Figure 7c), reaching the levels comparable to PAsp(DPT) (Figure 7b). The membrane destabilizing capacity of these polycations was further tested against HUVEC by a colorimetric LDH assay, in which the enzymatic activity of cytosolic LDH liberated from the cells was measured to estimate the membrane damages.[5,6] Figure 8a clearly shows that PAsp(DPT) induced LDH liberation in a concentration-dependent manner, both at acidic and physiological pH conditions. These data suggest a strong capacity of PAsp(DPT) to destabilize the endosomal membrane as well as the cytoplasmic membrane, regardless of the environmental pH. This is consistent with the results of the hemolysis assay shown in Figure 7b. Alternatively, the activity of LDH liberated from HUVEC incubated with PAsp(DET) was obviously low at pH 7.4, while the decrease in pH to acidic condition (pH ~5) substantially enhanced its activity to the same level as that of PAsp(DPT) (Figure 8b), exhibiting the similar trend to the hemolytic activity (Figure 7c). Similar results of the membrane destabilization were obtained for Huh-7 cells (data not shown). Apparently, the concentration-dependent increase in the membrane destabilization capacity of PAsp(DET) under the acidic condition corresponds to the enhanced transfection efficacy with N/P ratios (Figure 4).

We next sought to find a correlation between the interaction of the polycations with the membrane and the destabilization effect. CLSM observations were further carried out for HUVEC

(28) Zhang, Z.-Y.; Smith, B. D. *Bioconjugate Chem.* **2000**, *11*, 805–814.
(29) Merdan, T.; Kunath, K.; Fischer, D.; Kopecek, J.; Kissel, T. *Pharm. Res.* **2002**, *19*, 140–146.
(30) Bieber, T.; Meissner, W.; Kostin, S.; Niemann, A.; Elsasser, H.-P. *J. Controlled Release* **2002**, *82*, 441–454.
(31) Walker, G. F.; Fella, C.; Pelisek, J.; Fahrmeir, J.; Boeckle, S.; Ogris, M.; Wagner, E. *Mol. Ther.* **2005**, *11*, 418–425.

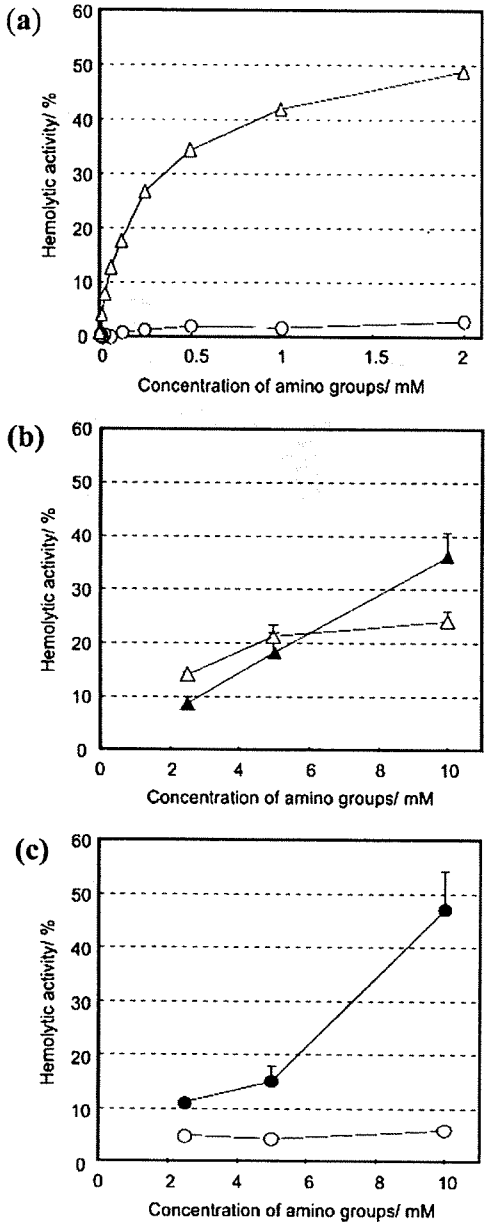

Figure 7. Hemolytic activity of PAsp(DET) and PAsp(DPT) against murine erythrocytes. (a) Hemolytic activity of PAsp(DET) (○) and PAsp(DPT) (△) after overnight erythrocyte incubation at pH 7.4 and 37 °C. (b) Hemolytic activity of PAsp(DPT) after 3 h incubation at pH 7.4 (△) and 5.5 (▲) (at 37 °C). (c) Hemolytic activity of PAsp(DET) after 3 h incubation at pH 7.4 (○) and 5.5 (●) (at 37 °C). Results were expressed as mean ± SEM ($n = 4$).

incubated with RhoB-labeled polycations. Fluorescence from PAsp(DET)−RhoB was not observed at pH 7.4 (Figure 9a) but upon acidic conditions (pH ~5), the fluorescence intensity was significant, extending to the cell periphery (Figure 9b), thereby indicating the appreciable cellular association of PAsp(DET)−RhoB at the acidic pH. In addition, CLSM studies with PAsp(DPT)−RhoB clearly showed significant levels of fluorescence at both pH's (Figure 9c,d), indicating a strong associative behavior of PAsp(DPT)−RhoB to cellular membrane, regardless of the pH. These images are in good agreement with the membrane-destabilizing capacity of the polycations determined by the hemolysis and LDH assays (Figures 7 and 8). It is reasonable to conclude from these results that PAsp-

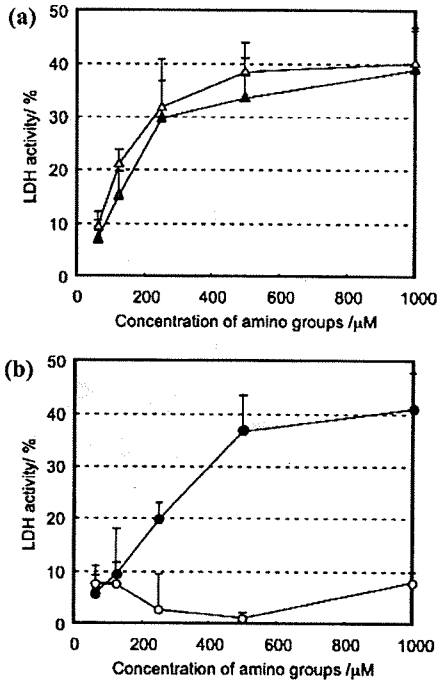

Figure 8. Enzymatic activity of LDH liberated from HUVEC upon interaction with the polycations at 37 °C for 1.5 h. (a) LDH activity for PAsp(DPT) system at pH 7.4 (△) and 5.5 (▲). (b) LDH activity for PAsp(DET) system at pH 7.4 (○) and 5.5 (●). Results were expressed as mean ± SEM ($n = 6$).

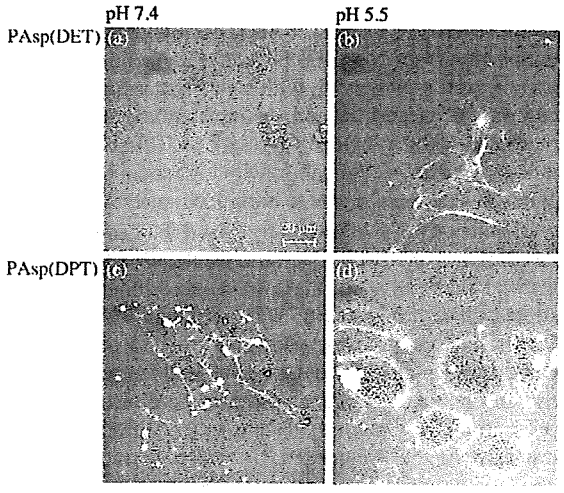

Figure 9. The adsorption of rhodamine B-labeled PAsp(DET) and PAsp(DPT) to HUVEC. The cells were incubated with the RhoB-labeled polycations (brightened as white) at the residual amino group concentration of 100 μM at 4 °C for 1 h, followed by washing with PBS, before CSLM imaging. (a) PAsp(DET) at pH 7.4, (b) PAsp(DET) at pH 5.5, (c) PAsp(DPT) at pH 7.4, (d) PAsp(DPT) at pH 5.5.

(DPT), without high buffering capacity (Figure 1), facilitates endosomal escape of its polyplexes into the cytoplasm through the direct perturbation of endosomal membrane. Nevertheless, the strong capacity of membrane destabilization, even at physiological pH, induces substantial damage to the cell membrane treated with PAsp(DPT) polyplexes as confirmed by the poor cell viability (Figure 5a,b). On the contrary, the weak interaction of PAsp(DET) with the plasma membrane at neutral pH is consistent with the lowered membrane-destabilizing capacity indicated from the results of hemolysis and LDH

assays. These data are supported by the high viability of the cells treated with PAsp(DET) polyplexes, as judged by MTT assay (Figures 5a,b). It should be further emphasized that the cellular association and the membrane-destabilizing capacity of PAsp(DET) were significantly enhanced by decreasing environmental pH to 5.5, becoming comparable to those of PAsp(DPT). This indicates that PAsp(DET) selectively destabilizes the membrane of the endosomal compartment with decreased pH to facilitate the endosomal escape of the polyplexes with minimal damage to the plasma membrane facing an extracellular pH of 7.4. Furthermore, it is reasonable to assume that cytoplasmic PAsp(DET) polyplexes may show minimal interaction with the membranes of organelles because of the pH recovery from acidic to neutral accompanied by the migration from the endosome to cytoplasm. Eventually, PAsp(DET) polyplexes successfully achieved the high transfection efficacy without impairing the cellular viability, as seen in Figure 4.

The unique pH dependency of the affinity of PAsp(DET) to cellular membrane is apparently correlated with the two-step protonation behavior of the flanking 1,2-diaminoethane unit in PAsp(DET). As described in the former section, the 1,2-diaminoethane unit assumes a monoprotonated gauche form at neutral pH, while additional protonation at an acidic pH induces a conformational transition to a diprotonated anti form (Scheme 1). This protonation change accompanying the conformational transition is likely related with the pH-modulated interaction of PAsp(DET) with the cellular membrane. Apparently, PAsp(DET) with the diamine unit in the monoprotonated gauche state exhibited a weak affinity for the cellular membrane but the diprotonated anti state revealed an increased affinity to perturb the membrane integrity. In contrast, the 1,3-diaminopropane unit in PAsp(DPT) assumes a diprotonated form at physiological, late endosomal, and lysosomal pH conditions; moreover, PAsp(DPT) shows a strong interaction with the cellular membrane, even at neutral pH conditions.

Conclusion

The present study was devoted to clarify key chemical parameters for the next generation of polycation/polyplexes exhibiting augmented levels of transfection efficacy and negligible cytotoxicity both in vitro and in vivo. This work primarily focused on N-substituted cationic poly(aspartamide) derivatives, PAsp(DET), possessing flanking 1,2-diaminoethane side chain, previously identified for effective in vivo transfection.[15,16] Comparative analysis between PAsp(DET) and PAsp(DPT) revealed that a single methylene unit difference in the diamine side chains had a crucial effect on the multiple cationic charge states. This seemingly minimal chemical change produced a striking contrast in their polyplex transfection behaviors, presumably due to the increased cytotoxicity. The high cytotoxicity of PAsp(DPT) was closely correlated to the degree of membrane destabilization, which was consistent with the strong interaction of PAsp(DPT) with the cellular membrane, even at physiological pH. The results of CLSM, hemolysis, and LDH analysis indicate that the membrane-destabilizing capacity of PAsp(DPT) contributes to the intracellular transport of PAsp(DPT) polyplexes, despite its weak buffering capacity. In contrast, the membrane destabilizing capacity of PAsp(DET) was highly altered, depending on the environmental pH. Two cationic charge states emerged with a monoprotonation at neutral pH and a diprotonated state at acidic conditions. We conclude that PAsp(DET) exhibits pH-selective membrane destabilization for late endosomal or lysosomal escape without compromising the membrane integrity of cytoplasmic vesicles and/or organelles. This unique approach provides the impetus for future nonviral gene vector development from synthetic poly(amino acids) with facile insertion of pH-selective membrane destabilizing structures to augment transfection efficacy and limit cytotoxicity. Thus, we show a novel and effective method to construct smart carrier systems useful for intracellular delivery of versatile bioactive components with inherently poor permeability to cellular membranes.

Acknowledgment. This work was financially supported by the Core Research Program for Evolutional Science and Technology (CREST) from the Japan Science and Technology Corp. (JST) as well as by Special Coordination Funds for Promoting Science and Technology from the Ministry of Education, Culture, Sports, Science and Technology of Japan (MEXT). The authors express their appreciation to Dr. H. Hamada (RIKEN, Japan) for providing the plasmid DNA and Dr. Darin Y Furgeson (University of Wisconsin—Madison) for proofreading of the manuscript. K. Miyata thanks the Research Fellowships of the Japan Society for the Promotion of Science for Young Scientists (JSPS) and the Mitsubishi Chemical Corp. Fund for their financial support.

Supporting Information Available: Experimental Section, Supporting Scheme 1, Supporting Figures 1−4, and Supporting Table 1. This material is available free of charge via the Internet at http://pubs.acs.org.

JA804561G

Pharmaceutical Research, Vol. 25, No. 12, December 2008 (© 2008)
DOI: 10.1007/s11095-008-9720-2

Research Paper

Polyplex Micelles from Triblock Copolymers Composed of Tandemly Aligned Segments with Biocompatible, Endosomal Escaping, and DNA-Condensing Functions for Systemic Gene Delivery to Pancreatic Tumor Tissue

Kanjiro Miyata,[1,6] Makoto Oba,[2] Mitsunobu R. Kano,[3,6] Shigeto Fukushima,[4] Yelena Vachutinsky,[1] Muri Han,[5] Hiroyuki Koyama,[2] Kohei Miyazono,[3,6] Nobuhiro Nishiyama,[4,6] and Kazunori Kataoka[1,4,5,6,7]

Received June 26, 2008; accepted August 26, 2008; published online September 10, 2008

Purpose. For systemic gene delivery to pancreatic tumor tissues, we prepared a three-layered polyplex micelle equipped with biocompatibility, efficient endosomal escape, and pDNA condensation functions from three components tandemly aligned; poly(ethylene glycol) (PEG), a poly(aspartamide) derivative with a 1,2-diaminoethane moiety (PAsp(DET)), and poly(L-lysine).
Materials and Methods. The size and *in vitro* transfection efficacy of the polyplex micelles were determined by dynamic light scattering (DLS) and luciferase assay, respectively. The systemic gene delivery with the polyplex micelles was evaluated from enhanced green fluorescence protein (EGFP) expression in the tumor tissues.
Results. The polyplex micelles were approximately 80 nm in size and had one order of magnitude higher *in vitro* transfection efficacy than that of a diblock copolymer as a control. With the aid of transforming growth factor (TGF)-β type I receptor (TβR-1) inhibitor, which enhances accumulation of macromolecular drugs in tumor tissues, the polyplex micelle from the triblock copolymer showed significant EGFP expression in the pancreatic tumor (BxPC3) tissues, mainly in the stromal regions including the vascular endothelial cells and fibroblasts.
Conclusion. The three-layered polyplex micelles were confirmed to be an effective gene delivery system to subcutaneously implanted pancreatic tumor tissues through systemic administration.

KEY WORDS: gene delivery; PEG; polyplex micelle; TGF-β inhibitor; triblock copolymer.

INTRODUCTION

Successful gene delivery through systemic administration is crucial for the gene therapy of various intractable diseases, including cancer. Use of an appropriate gene vector is needed for systemic administration to achieve selective accumulation of the intact gene in target tissues, and subsequently, to reveal effective gene expression with a sufficient therapeutic index. Although major gene vectors in clinical trials are viral-based systems (1), they could have risks of immunogenicity and mutagenicity that would interfere with their practical use in clinics. Synthetic polymer-based vectors (polyplexes) are attractive alternatives of viruses, because of much lower immunogenicity, greater ease of chemical modification and larger-scale preparation (2–4). To attain successful transfection in tumor tissues *via* intravenous administration by polyplex vectors, several important issues as follows should be addressed: (1) high stability to protect the DNA structure in the biological milieu from nuclease attack, (2) minimized non-specific interaction with biological components to exert longevity in the blood circulation, and (3) smooth escape from endosomes to cytoplasm for efficient gene expression inside target cells.

To fulfill such requirements, polyplexes with poly(ethylene glycol) (PEG) palisades (polyplex micelle) have been prepared by several groups including ourselves through the self-assembly of PEG-polycation copolymers with plasmid DNA (pDNA) (4–8). Indeed, polyplex micelles prepared from PEG–poly(L-lysine) block copolymer (PEG–PLys) showed high tolerability in serum media (9), allowing for a prolonged circulation period of intact pDNA in the blood stream, whereas naked pDNA was completely digested within

[1] Department of Bioengineering, Graduate School of Engineering, The University of Tokyo, 7-3-1 Hongo, Bunkyo-ku, Tokyo, 113-8656, Japan.
[2] Department of Clinical Vascular Regeneration, Graduate School of Medicine, The University of Tokyo, 7-3-1 Hongo, Bunkyo-ku, Tokyo, 113-8655, Japan.
[3] Department of Molecular Pathology, Graduate School of Medicine, The University of Tokyo, 7-3-1 Hongo, Bunkyo-ku, Tokyo, 113-8655, Japan.
[4] The Center for Disease Biology and Integrative Medicine, Graduate School of Medicine, The University of Tokyo, 7-3-1 Hongo, Bunkyo-ku, Tokyo, 113-0033, Japan.
[5] Department of Materials Engineering, Graduate School of Engineering, 7-3-1 Hongo, Bunkyo-ku, Tokyo, 113-8656, Japan.
[6] Center for NanoBio Integration, The University of Tokyo, 7-3-1 Hongo, Bunkyo-ku, Tokyo, 113-8656, Japan.
[7] To whom correspondence should be addressed. (e-mail: kataoka@bmw.t.u-tokyo.ac.jp)

0724-8741/08/1200-2924/0

5 min (10). Nevertheless, PLys-based systems have encountered the issue of inefficient transfection activity, because of the lack of endosome escape, involving a "proton sponge effect" caused by amino groups with a low pKa value as typically reported in poly(ethylenimine) (PEI)-based systems (11,12). Worth noting in this regard is our recent finding that polyplexes from a poly(aspartamide) derivative having 1,2-diaminoethane unit as a side chain, poly{*N*-[*N*-(2-aminoethyl)-2-aminoethyl]aspartamide} (PAsp(DET)), revealed highly efficient transfection with minimal cytotoxicity to a variety of cells including primary cells (13–16), probably due to facilitated endosomal escape based on remarkable change in the protonation degree between physiological pH and endosomal acidic pH. Actually, the PEG–PAsp(DET) polyplex micelle succeeded in *in vivo* transfection of a reporter gene (luciferase) to a rabbit's clamped carotid artery *via* intra-arterial injection (17). Also, when the PEG–PAsp(DET) polyplex micelle was incorporated into a calcium phosphate cement scaffold and then applied in a bone defect model to a mouse skull bone, substantial bone formation surrounding the entire lower surface of the implant was induced by the regulated release of the micelles containing a constitutively active form of activin receptor-like kinase 6 (caALK6) and runt-related transcription factor 2 (Runx2) genes from the scaffold (18). The relatively weak affinity of PAsp(DET) segments to pDNA (19) is also an advantage for the smooth release of the incorporated pDNA and subsequent efficient transcription in the cell interior. On the other hand, such weak affinity probably leads to the detachment of PAsp (DET) chains from pDNA in the polyplex micelle through the interaction with biological components during circulation in the blood stream, resulting in a loss of transfection activity. Therefore, strategies to stabilize the structure of the polyplex micelles against PEG–PAsp(DET) are needed for the development of effective systemic administration methods.

The present study was devoted to develop a PEG–PAsp (DET)-based polyplex micelle for systemic use by conjugating a PLys segment as an anchoring moiety to pDNA at the ω-end of the diblock copolymer. For this purpose, a triblock copolymer of poly(ethylene glycol)-poly{*N*-[*N*-(2-aminoethyl)-2-aminoethyl]aspartamide}-poly(L-lysine) (PEG–PAsp (DET)–PLys) was prepared to integrate three functional segments engendering biocompatibility (PEG), efficient endosomal escape (PAsp(DET)), and effective pDNA condensation (PLys), respectively. In this way, three-layered polyplex micelles can be constructed, in which the middle layer, functioning as an endosomal escape element, is sandwiched between an outer layer of biocompatible PEG and an inner layer of PLys/pDNA polyplex (20). The fluorescence measurement with an intercalator into DNA indicated that pDNA mixed with the triblock copolymers was condensed more tightly than in a PEG–PAsp(DET) diblock copolymer and comparably to a PEG–PLys diblock copolymer. Intracellular trafficking of the polyplex micelles with or without the intermediate layer of PAsp(DET) was compared in detail by confocal fluorescence microscopy to reveal the endosomal escape of the micelles with the PAsp(DET) layer. Finally, reporter gene expression in a subcutaneous pancreatic tumor model, representing an intractable solid tumor with thick fibrosis and hypovascularity, demonstrated that the intravenously injected three-layered polyplex micelles effectively penetrated tumor vasculature in combination with transforming growth factor (TGF)-β type I receptor inhibitor (TβR-I) (21).

MATERIALS AND METHODS

Materials

α-Methoxy-ω-amino-poly(ethylene glycol) (Mw 12,000; PEG–NH_2) and β-benzyl-L-aspartate *N*-carboxy-anhydride (BLA–NCA) were obtained from Nippon Oil and Fats Co., Ltd. (Tokyo, Japan). ε-(Benzyloxycarbonyl)-L-lysine *N*-carboxy anhydride (Lys(Z))–NCA was synthesized from ε-(benzyloxycarbonyl)-L-lysine (Wako Pure Chemical Industries, Ltd., Osaka, Japan) by the Fuchs-Farthing method using bis(trichloromethyl) carbonate (triphosgene; Tokyo Kasei Kogyo Co., Ltd., Tokyo, Japan) (22). Diethylenetriamine (DET; bis(2-aminoethyl)amine), *N*,*N*-dimethylformamide (DMF), dichloromethane, benzene, trifluoroacetic acid, *N*-methyl 2-pyrrolidone (NMP), Tris (tris(hydroxymethyl) aminomethane) and HEPES (2-[4-(2-hydroxyethyl)-1-piperazinyl]ethanesulfonic acid) were purchased from Wako Pure Chemical Industries, Ltd., Osaka, Japan. DMF and dichloromethane distilled by conventional methods were used for the polymer synthesis. DET was distilled over CaH_2 under reduced pressure, and then used for the aminolysis reaction. A pDNA coding for luciferase with a CAG promoter provided by RIKEN (Japan) was used after the amplification in competent DH5α *Escherichia coli* and the subsequent purification using a HiSpeed Plasmid MaxiKit purchased from QIAGEN Science Co., Inc. (Germantown, MD, USA). A full-size Label IT Cy5 Labeling Kit was purchased from Mirus Bio Corporation (Madison, WI, USA). Twenty-four- and 96-well culture plates were purchased from Becton Dickinson Labware (Franklin Lakes, NJ, USA). A human hepatocyte, Huh-7, was obtained from the RIKEN Cell Bank (RIKEN Bioresource Center, Japan). A human pancreatic adenocarcinoma cell line, BxPC3, was obtained from the American Type Culture Collection (Manassas, VA, USA). Dulbecco's Modified Eagle's Medium (DMEM) and RPMI medium 1640 were purchased from Sigma-Aldrich Co. (St. Louis, MO, USA). Fetal bovine serum (FBS) was purchased from Dainippon Sumitomo Parma Co., Ltd. (Osaka, Japan). A Luciferase Assay System Kit was purchased from Promega Co. (Madison, WI, USA), and a Micro BCA™ Protein Assay Reagent Kit was purchased from Pierce Co., Inc. (Rockford, IL, USA). TβR-I inhibitor was purchased from Calbiochem (San Diego, CA, USA; LY364947; catalog no. 616451). Rat monoclonal antibody anti-platelet endothelial cell adhesion molecule-1 (PECAM-1), as a marker for vascular endothelial cells, was purchased from BD Pharmingen (Franklin Lakes, NJ, USA), and Alexa647-conjugated secondary antibody to rat IgG was from Invitrogen Molecular Probes (Eugene, OR, USA).

Synthesis of PEG–PBLA–PLys(Z) Triblock Copolymer

A triblock copolymer, PEG–PBLA–PLys(Z), was synthesized as previously described (20). Briefly, the PEG–poly (β-benzyl L-aspartate) diblock copolymer (PEG–PBLA) was synthesized by the ring-opening polymerization of BLA–NCA initiated by PEG–NH_2, followed by the additional ring-